












# TECH BRIEFS

NATIONAL AERONAUTICS AND SPACE ADMINISTRATION

-  Technology Focus
-  Electronics/Computers
-  Software
-  Materials
-  Mechanics/Machinery
-  Manufacturing
-  Bio-Medical
-  Physical Sciences
-  Information Sciences
-  Books and Reports
-  Green Design



# INTRODUCTION

Tech Briefs are short announcements of innovations originating from research and development activities of the National Aeronautics and Space Administration. They emphasize information considered likely to be transferable across industrial, regional, or disciplinary lines and are issued to encourage commercial application.

## Availability of NASA Tech Briefs and TSPs

Requests for individual Tech Briefs or for Technical Support Packages (TSPs) announced herein should be addressed to

### National Technology Transfer Center

Telephone No. **(800) 678-6882** or via World Wide Web at **[www.nttc.edu](http://www.nttc.edu)**

Please reference the control numbers appearing at the end of each Tech Brief. Information on NASA's Innovative Partnerships Program (IPP), its documents, and services is also available at the same facility or on the World Wide Web at **<http://www.nasa.gov/offices/ipp/network/index.html>**

Innovative Partnerships Offices are located at NASA field centers to provide technology-transfer access to industrial users. Inquiries can be made by contacting NASA field centers listed below.

Ames Research Center  
Lisa L. Lockyer  
(650) 604-1754  
[lisa.l.lockyer@nasa.gov](mailto:lisa.l.lockyer@nasa.gov)

Dryden Flight Research Center  
Yvonne D. Gibbs  
(661) 276-3720  
[yvonne.d.gibbs@nasa.gov](mailto:yvonne.d.gibbs@nasa.gov)

Glenn Research Center  
Kathy Needham  
(216) 433-2802  
[kathleen.k.needham@nasa.gov](mailto:kathleen.k.needham@nasa.gov)

Goddard Space Flight Center  
Nona Cheeks  
(301) 286-5810  
[nona.k.cheeks@nasa.gov](mailto:nona.k.cheeks@nasa.gov)

Jet Propulsion Laboratory  
Andrew Gray  
(818) 354-4906  
[gray@jpl.nasa.gov](mailto:gray@jpl.nasa.gov)

Johnson Space Center  
information  
(281) 483-3809  
[jsc.techtran@mail.nasa.gov](mailto:jsc.techtran@mail.nasa.gov)

Kennedy Space Center  
David R. Makufka  
(321) 867-6227  
[david.r.makufka@nasa.gov](mailto:david.r.makufka@nasa.gov)

Langley Research Center  
Elizabeth B. Plentovich  
(757) 864-2857  
[elizabeth.b.plentovich@nasa.gov](mailto:elizabeth.b.plentovich@nasa.gov)

Marshall Space Flight Center  
Jim Dowdy  
(256) 544-7604  
[jim.dowdy@msfc.nasa.gov](mailto:jim.dowdy@msfc.nasa.gov)

Stennis Space Center  
Ramona Travis  
(228) 688-3832  
[ramona.e.travis@nasa.gov](mailto:ramona.e.travis@nasa.gov)

Carl Ray, Program Executive  
Small Business Innovation  
Research (SBIR) & Small  
Business Technology  
Transfer (STTR) Programs  
(202) 358-4652  
[carl.g.ray@nasa.gov](mailto:carl.g.ray@nasa.gov)

Doug Comstock, Director  
Innovative Partnerships  
Program Office  
(202) 358-2221  
[doug.comstock@nasa.gov](mailto:doug.comstock@nasa.gov)



# TECH BRIEFS

NATIONAL AERONAUTICS AND SPACE ADMINISTRATION

## 5 Technology Focus: Sensors

- 5 Distributed Aerodynamic Sensing and Processing Toolbox
- 5 Collaborative Supervised Learning for Sensor Networks
- 5 Hazard Detection Software for Lunar Landing
- 6 Onboard Nonlinear Engine Sensor and Component Fault Diagnosis and Isolation Scheme
- 6 Network-Capable Application Process and Wireless Intelligent Sensors for ISHM

## 9 Semiconductors & ICs

- 9 Interface Supports Multiple Broadcast Transceivers for Flight Applications
- 9 FPGA Sequencer for Radar Altimeter Applications
- 9 Miniature Sapphire Acoustic Resonator — MSAR
- 10 Process-Hardened, Multi-Analyte Sensor for Characterizing Rocket Plume Constituents
- 10 SAD5 Stereo Correlation Line-Striping in an FPGA

## 13 Manufacturing & Prototyping

- 13 Hybrid Composite Cryogenic Tank Structure
- 13 Nanoscale Deformable Optics
- 14 Reliability-Based Design Optimization of a Composite Airframe Component
- 14 Zinc Oxide Nanowire Interphase for Enhanced Lightweight Polymer Fiber Composites

## 17 Mechanics/Machinery

- 17 Plasma Igniter for Reliable Ignition of Combustion in Rocket Engines
- 17 Wire Test Grip Fixture
- 18 A Sub-Hertz, Low-Frequency Vibration Isolation Platform

## 19 Materials & Coatings

- 19 Carbon Nanofibers Synthesized on Selective Substrates for Nonvolatile Memory and 3D Electronics
- 20 Nanoparticle/Polymer Nanocomposite Bond Coat or Coating

## 21 Green Design

- 21 High-Resolution Wind Measurements for Offshore Wind Energy Development
- 21 Spring Tire

## 23 Software

- 23 Marsviewer 2008
- 23 Mission Services Evolution Center Message Bus
- 23 Major Constituents Analysis for the Vehicle Cabin Atmosphere Monitor
- 24 Astronaut Health Participant Summary Application
- 24 Adaption of the AMDIS Method to Flight Status on the VCAM Instrument
- 24 Natural Language Interface for Safety Certification of Safety-Critical Software

## 27 Physical Sciences

- 27 Cryogenic Caging for Science Instrumentation
- 27 Wide-Range Neutron Detector for Space Nuclear Applications
- 27 *In Situ* Guided Wave Structural Health Monitoring System
- 28 Multiplexed Energy Coupler for Rotating Equipment
- 28 Attitude Estimation in Fractionated Spacecraft Cluster Systems
- 28 Full Piezoelectric Multilayer-Stacked Hybrid Actuation/Transduction Systems
- 29 Active Flow Effectors for Noise and Separation Control
- 29 Method and System for Temporal Filtering in Video Compression Systems
- 30 Apparatus for Measuring Total Emissivity of Small, Low-Emissivity Samples
- 30 Multiple-Zone Diffractive Optic Element for Laser Ranging Applications
- 31 Simplified Architecture for Precise Aiming of a Deep-Space Communication Laser Transceiver
- 32 Two-Photon-Absorption Scheme for Optical Beam Tracking
- 32 High-Sensitivity, Broad-Range Vacuum Gauge Using Nanotubes for Micromachined Cavities

This document was prepared under the sponsorship of the National Aeronautics and Space Administration. Neither the United States Government nor any person acting on behalf of the United States Government assumes any liability resulting from the use of the information contained in this document, or warrants that such use will be free from privately owned rights.

- 33 Wide-Field Optic for Autonomous Acquisition of Laser Link
- 34 Extracting Zero-Gravity Surface Figure of a Mirror

### **35 Information Sciences**

- 35 Modeling Electromagnetic Scattering From Complex Inhomogeneous Objects
- 35 Visual Object Recognition and Tracking of Tools
- 36 Method for Implementing Optical Phase Adjustment
- 36 Visual SLAM Using Variance Grid Maps
- 37 Rapid Calculation of Spacecraft Trajectories Using Efficient Taylor Series Integration
- 37 Efficient Kriging Algorithms WeavEncke Method

- 37 Predicting Spacecraft Trajectories by the WeavEncke Method
- 38 An Augmentation of G-Guidance Algorithms
- 38 Comparison of Aircraft Icing Growth Assessment Software

### **41 Books & Reports**

- 41 Silicon-Germanium Voltage-Controlled Oscillator at 105 GHz
- 41 Estimation of Coriolis Force and Torque Acting on Ares-1
- 41 Null Lens Assembly for X-Ray Mirror Segments
- 41 High-Precision Pulse Generator





### ➊ Distributed Aerodynamic Sensing and Processing Toolbox

*Dryden Flight Research Center, Edwards, California*

A Distributed Aerodynamic Sensing and Processing (DASP) toolbox was designed and fabricated for flight test applications with an Aerostructures Test Wing (ATW) mounted under the fuselage of an F-15B on the Flight Test Fixture (FTF). DASP monitors and processes the aerodynamics with the structural dynamics using nonintrusive, surface-mounted, hot-film sensing. This aerodynamic measurement tool benefits programs devoted to static/dynamic load alleviation, body freedom flutter suppression, buffet control, improve-

ment of aerodynamic efficiency through cruise control, supersonic wave drag reduction through shock control, etc.

This DASP toolbox measures local and global unsteady aerodynamic load distribution with distributed sensing. It determines correlation between aerodynamic “observables” (aero forces) and structural dynamics, and allows control authority increase through aeroelastic shaping and active flow control.

It offers improvements in flutter suppression and, in particular, body free-

dom flutter suppression, as well as aerodynamic performance of wings for increased range/endurance of manned/unmanned flight vehicles. Other improvements include inlet performance with closed-loop active flow control, and development and validation of advanced analytical and computational tools for unsteady aerodynamics.

*This work was done by Martin Brenner and Christine Jutte of Dryden Flight Research Center and Arun Mangalam of Tao Systems, Inc. Further information is contained in a TSP (see page 1). DRC-009-031*

### ➋ Collaborative Supervised Learning for Sensor Networks This technique could be applied to sensor networks for intruder detection, target tracking, and data mining in cell-phone networks.

*NASA's Jet Propulsion Laboratory, Pasadena, California*

Collaboration methods for distributed machine-learning algorithms involve the specification of communication protocols for the learners, which can query other learners and/or broadcast their findings preemptively. Each learner incorporates information from its neighbors into its own training set, and they are thereby able to “bootstrap” each other to higher performance.

Each learner resides at a different node in the sensor network and makes observations (collects data) independently of the other learners. After being “seeded” with an initial labeled training set, each learner proceeds to learn in an iterative fashion. New data is collected and classified. The learner can then ei-

ther broadcast its most confident classifications for use by other learners, or can query neighbors for their classifications of its least confident items. As such, collaborative learning combines elements of both passive (broadcast) and active (query) learning. It also uses ideas from ensemble learning to combine the multiple responses to a given query into a single useful label.

This approach has been evaluated against current non-collaborative alternatives, including training a single classifier and deploying it at all nodes with no further learning possible, and permitting learners to learn from their own most confident judgments, absent interaction with their neighbors. On several

data sets, it has been consistently found that active collaboration is the best strategy for a distributed learner network. The main advantages include the ability for learning to take place autonomously by collaboration rather than by requiring intervention from an oracle (usually human), and also the ability to learn in a distributed environment, permitting decisions to be made *in situ* and to yield faster response time.

*This work was done by Kiri L. Wagstaff of Caltech, Umaa Rebbapragada of Tufts University, and Terran Lane of the University of New Mexico for NASA's Jet Propulsion Laboratory. For more information, contact iaofice@jpl.nasa.gov. NPO-46914*

### ➌ Hazard Detection Software for Lunar Landing

*NASA's Jet Propulsion Laboratory, Pasadena, California*

The Autonomous Landing and Hazard Avoidance Technology (ALHAT) Project is developing a system for safe and precise manned lunar landing that involves novel sensors, but also specific

algorithms. ALHAT has selected imaging LIDAR (light detection and ranging) as the sensing modality for onboard hazard detection because imaging LIDARs can rapidly generate direct meas-

urements of the lunar surface elevation from high altitude. Then, starting with the LIDAR-based Hazard Detection and Avoidance (HDA) algorithm developed for Mars Landing, JPL has developed a

mature set of HDA software for the manned lunar landing problem.

Landing hazards exist everywhere on the Moon, and many of the more desirable landing sites are near the most hazardous terrain, so HDA is needed to autonomously and safely land payloads over much of the lunar surface. The HDA requirements used in the ALHAT project are to detect hazards that are 0.3 m tall or higher and slopes that are 5° or greater. Steep slopes, rocks, cliffs, and gullies are all hazards for landing and, by computing the local slope and roughness in an elevation map, all of these hazards can be detected. The algorithm in this innovation is used to measure slope and roughness hazards. In addition

to detecting these hazards, the HDA capability also is able to find a safe landing site free of these hazards for a lunar lander with diameter ≈15 m over most of the lunar surface.

This software includes an implementation of the HDA algorithm, software for generating simulated lunar terrain maps for testing, hazard detection performance analysis tools, and associated documentation. The HDA software has been deployed to Langley Research Center and integrated into the POST II Monte Carlo simulation environment. The high-fidelity Monte Carlo simulations determine the required ground spacing between LIDAR samples (ground sample distances) and the

noise on the LIDAR range measurement. This simulation has also been used to determine the effect of viewing on hazard detection performance. The software has also been deployed to Johnson Space Center and integrated into the ALHAT real-time Hardware-in-the-Loop testbed.

*This work was done by Andres Huertas, Andrew E. Johnson, Robert A. Werner, and James F. Montgomery of Caltech for NASA's Jet Propulsion Laboratory. For more information, contact iaoffice@jpl.nasa.gov.*

*This software is available for commercial licensing. Please contact Daniel Broderick of the California Institute of Technology at danielb@caltech.edu. Refer to NPO-47178.*

---

## Onboard Nonlinear Engine Sensor and Component Fault Diagnosis and Isolation Scheme

*John H. Glenn Research Center, Cleveland, Ohio*

A method detects and isolates in-flight sensor, actuator, and component faults for advanced propulsion systems. In sharp contrast to many conventional methods, which deal with either sensor fault or component fault, but not both, this method considers sensor fault, actuator fault, and component fault under one systemic and unified framework.

The proposed solution consists of two main components: a bank of real-time, nonlinear adaptive fault diagnostic estimators for residual generation, and a residual evaluation module that includes adaptive thresholds and a Trans-

ferable Belief Model (TBM)-based residual evaluation scheme. By employing a nonlinear adaptive learning architecture, the developed approach is capable of directly dealing with nonlinear engine models and nonlinear faults without the need of linearization. Software modules have been developed and evaluated with the NASA C-MAPSS engine model. Several typical engine-fault modes, including a subset of sensor/actuator/components faults, were tested with a mild transient operation scenario. The simulation results demonstrated that the algorithm was able to success-

fully detect and isolate all simulated faults as long as the fault magnitudes were larger than the minimum detectable/isolable sizes, and no misdiagnosis occurred.

*This work was done by Liang Tang and Jonathan A. DeCastro of Impact Technologies, LLC and Xiaodong Zhang of Wright State University for Glenn Research Center.*

*Inquiries concerning rights for the commercial use of this invention should be addressed to NASA Glenn Research Center, Innovative Partnerships Office, Attn: Steve Fedor, Mail Stop 4-8, 21000 Brookpark Road, Cleveland, Ohio 44135. Refer to LEW-18518-1/9-1.*

---

## Network-Capable Application Process and Wireless Intelligent Sensors for ISHM

**This technology can be used for wireless sensor monitoring in vehicles, home security, system automation, and radio-frequency identification (RFID) for smart tags.**

*Stennis Space Center, Mississippi*

Intelligent sensor technology and systems are increasingly becoming attractive means to serve as frameworks for intelligent rocket test facilities with embedded intelligent sensor elements, distributed data acquisition elements, and onboard data acquisition elements. Networked intelligent processors enable users and systems integrators to automatically configure their measurement automation

systems for analog sensors. NASA and leading sensor vendors are working together to apply the IEEE 1451 standard for adding plug-and-play capabilities for wireless analog transducers through the use of a Transducer Electronic Data Sheet (TEDS) in order to simplify sensor setup, use, and maintenance, to automatically obtain calibration data, and to eliminate manual data entry and error.

A TEDS contains the critical information needed by an instrument or measurement system to identify, characterize, interface, and properly use the signal from an analog sensor. A TEDS is deployed for a sensor in one of two ways. First, the TEDS can reside in embedded, nonvolatile memory (typically flash memory) within the intelligent processor. Second, a virtual TEDS can exist as a



separate file, downloadable from the Internet. This concept of virtual TEDS extends the benefits of the standardized TEDS to legacy sensors and applications where the embedded memory is not available. An HTML-based user interface provides a visual tool to interface with those distributed sensors that a TEDS is associated with, to automate the sensor management process.

Implementing and deploying the IEEE 1451.1-based Network-Capable Application Process (NCAP) can achieve support for intelligent process in Integrated Systems Health Management (ISHM) for the purpose of monitoring, detection of anomalies, diagnosis of causes of anomalies, prediction of future anomalies, mitigation to maintain operability, and integrated awareness of system health by the operator. It can also support local data collection and storage. This invention enables wide-area sensing and employs numerous globally

distributed sensing devices that observe the physical world through the existing sensor network. This innovation enables distributed storage, distributed processing, distributed intelligence, and the availability of DiaK (Data, Information, and Knowledge) to any element as needed. It also enables the simultaneous execution of multiple processes, and represents models that contribute to the determination of the condition and health of each element in the system.

The NCAP (intelligent process) can configure data-collection and filtering processes in reaction to sensed data, allowing it to decide when and how to adapt collection and processing with regard to sophisticated analysis of data derived from multiple sensors. The user will be able to view the sensing device network as a single unit that supports a high-level query language. Each query would be able to operate over data collected from across the global sensor net-

work just as a search query encompasses millions of Web pages.

The sensor web can preserve ubiquitous information access between the querier and the queried data. Pervasive monitoring of the physical world raises significant data and privacy concerns. This innovation enables different authorities to control portions of the sensing infrastructure, and sensor service authors may wish to compose services across authority boundaries.

*This work was done by Fernando Figueroa, Jon Morris, and Mark Turowski of Stennis Space Center and Ray Wang of Mobitrum Corp. Inquiries concerning rights for the commercial use of this invention should be addressed to:*

*Ray Wang  
Mobitrum Corporation  
8070 Georgia Avenue, Suite 209  
Silver Spring, MD 20910  
(301) 585-4040  
Refer to SSC-00313/5.*





### **Interface Supports Multiple Broadcast Transceivers for Flight Applications**

*NASA's Jet Propulsion Laboratory, Pasadena, California*

A wireless avionics interface provides a mechanism for managing multiple broadcast transceivers. This interface isolates the control logic required to support multiple transceivers so that the flight application does not have to manage wireless transceivers. All of the logic to select transceivers, detect transmitter and receiver faults, and take autonomous recovery action is contained in the interface, which is not restricted to using wireless transceivers. Wired, wireless, and mixed transceiver technologies are supported.

This design's use of broadcast data technology provides inherent cross-

strapping of data links. This greatly simplifies the design of redundant flight subsystems. The interface fully exploits the broadcast data link to determine the health of other transceivers used to detect and isolate faults for fault recovery. The interface uses simplified control logic, which can be implemented as an intellectual-property (IP) core in a field-programmable gate array (FPGA).

The interface arbitrates the reception of inbound data traffic appearing on multiple receivers. It arbitrates the transmission of outbound traffic. This system also monitors broadcast data traffic to determine the health of transmitters in

the network, and then uses this health information to make autonomous decisions for routing traffic through transceivers. Multiple selection strategies are supported, like having an active transceiver with the secondary transceiver powered off except to send periodic health status reports. Transceivers can operate in round-robin for load-sharing and graceful degradation.

*This work was done by Gary L. Block, William D. Whitaker, James W. Dillon, James P. Lux, and Mohammad Ahmad of Caltech for NASA's Jet Propulsion Laboratory. For more information, contact [iaoffice@jpl.nasa.gov](mailto:iaoffice@jpl.nasa.gov). NPO-46317*

### **FPGA Sequencer for Radar Altimeter Applications**

*NASA's Jet Propulsion Laboratory, Pasadena, California*

A sequencer for a radar altimeter provides accurate attitude information for a reliable soft landing of the Mars Science Laboratory (MSL). This is a field-programmable-gate-array (FPGA)-only implementation. A table loaded externally into the FPGA controls timing, processing, and decision structures. Radar is memory-less and does not use previous acquisitions to assist in the current acquisition. All cycles complete in exactly 50 milliseconds, regardless of range or whether a target was found.

A RAM (random access memory) within the FPGA holds instructions for up to 15 sets. For each set, timing is run, echoes are processed, and a comparison is made. If a target is seen, more detailed processing is run on that set. If no target is seen, the next set is tried.

When all sets have been run, the FPGA terminates and waits for the next 50-millisecond event. This setup simplifies testing and improves reliability. A single vertex chip does the work of an entire assembly. Output products re-

quire minor processing to become range and velocity.

This technology is the heart of the Terminal Descent Sensor, which is an integral part of the Entry Decent and Landing system for MSL. In addition, it is a strong candidate for manned landings on Mars or the Moon.

*This work was done by Andrew C. Berkun, Brian D. Pollard, and Curtis W. Chen of Caltech for NASA's Jet Propulsion Laboratory. For more information, contact [iaoffice@jpl.nasa.gov](mailto:iaoffice@jpl.nasa.gov). NPO-46988*

### **Miniature Sapphire Acoustic Resonator — MSAR**

**Q values as high as  $10^8$  may be achieved at room temperature.**

*NASA's Jet Propulsion Laboratory, Pasadena, California*

A room temperature sapphire acoustics resonator incorporated into an oscillator represents a possible opportunity to improve on quartz ultra-stable oscillator (USO) performance, which has been a staple for NASA missions since the inception of spaceflight.

Where quartz technology is very mature and shows a performance improvement of perhaps 1 dB/decade, these sapphire acoustic resonators when integrated with matured quartz electronics could achieve a frequency stability improvement of 10 dB or

more. As quartz oscillators are an essential element of nearly all types of frequency standards and reference systems, the success of MSAR would advance the development of frequency standards and systems for both ground-based and flight-based projects.

Current quartz oscillator technology is limited by quartz mechanical  $Q$ . With a possible improvement of more than  $\times 10$   $Q$  with sapphire acoustic modes, the stability limit of current quartz oscillators may be improved tenfold, to  $10^{-14}$  at 1 second. The electromagnetic modes of sapphire that were previously developed at JPL require cryogenic temperatures to achieve the high  $Q$  levels needed to achieve this stability level. However sapphire's acoustic modes, which have not been used before in a high-stability oscillator, indicate the required  $Q$  values (as high as  $Q = 10^8$ ) may be achieved at room temperature in the kHz range. Even though sapphire is not piezoelectric, such a high  $Q$  should allow electrostatic excitation of the acoustic modes with a combination of DC and AC voltages across a small sapphire disk ( $\approx 1$  mm thick). The first evaluations under this task will test predictions of an estimated input impedance of 10 kilohms at  $Q = 10^8$ , and explore the  $Q$  values that can be realized in a smaller resonator, which

has not been previously tested for acoustic modes.

This initial  $Q$  measurement and excitation demonstration can be viewed similar to a transducer converting electrical energy to mechanical energy and back. Such an electrostatic tweeter type excitation of a mechanical resonator will be tested at 5 MHz. Finite element calculation will be applied to resonator design for the desired resonator frequency and optimum configuration. The experiment consists of the sapphire resonator sandwiched between parallel electrodes. A DC+AC voltage can be applied to generate a force to act on a sapphire resonator. With the frequency of the AC voltage tuned to the sapphire resonator frequency, a resonant condition occurs and the sapphire  $Q$  can be measured with a high-frequency impedance analyzer.

To achieve high  $Q$  values, many experimental factors such as vacuum seal, gas damping effects, charge buildup on the sapphire surface, heat dissipation, sapphire anchoring, and the sapphire

mounting configuration will need attention. The effects of these parameters will be calculated and folded into the resonator design. It is envisioned that the initial test configuration would allow for movable electrodes to check gap spacing dependency and verify the input impedance prediction.

Quartz oscillators are key components in nearly all ground- and space-based communication, tracking, and radio science applications. They play a key role as local oscillators for atomic frequency standards and serve as flywheel oscillators or to improve phase noise in high-performance frequency and timing distribution systems. With ultra-stable performance from one to three seconds, an Earth-orbit or moon-based MSAR can enhance available performance options for spacecraft due to elimination of atmospheric path degradation.

*This work was done by Rabi T. Wang and Robert L. Tjoelker of Caltech for NASA's Jet Propulsion Laboratory For more information, contact iaoffice@jpl.nasa.gov. NPO-47343*

---

## Process-Hardened, Multi-Analyte Sensor for Characterizing Rocket Plume Constituents

*Stennis Space Center, Mississippi*

A multi-analyte sensor was developed that enables simultaneous detection of rocket engine combustion-product molecules in a launch-vehicle ground test stand. The sensor was developed using a pin-printing method by incorporating multiple sensor elements on a single chip. It demonstrated accurate and sensitive detection of analytes such as carbon dioxide, carbon monoxide, kerosene,

isopropanol, and ethylene from a single measurement.

The use of pin-printing technology enables high-volume fabrication of the sensor chip, which will ultimately eliminate the need for individual sensor calibration since many identical sensors are made in one batch. Tests were performed using a single-sensor chip attached to a fiber-optic bundle. The use

of a fiber bundle allows placement of the opto-electronic readout device at a place remote from the test stand. The sensors are rugged for operation in harsh environments.

*This work was done by Kisholoy Goswami for Stennis Space Center. For more information, contact: Kisholoy Goswami, InnoSense, LLC; (310) 530-2011. SSC-00348*

---

## SAD5 Stereo Correlation Line-Striping in an FPGA

*NASA's Jet Propulsion Laboratory, Pasadena, California*

High precision SAD5 stereo computations can be performed in an FPGA (field-programmable gate array) at much higher speeds than possible in a conventional CPU (central processing unit), but this uses large amounts of FPGA resources that scale with image size. Of the two key resources in an FPGA, Slices and BRAM (block RAM), Slices scale linearly in the new algorithm with image size, and BRAM scales quadratically with image size. An approach

was developed to trade latency for BRAM by sub-windowing the image vertically into overlapping strips and stitching the outputs together to create a single continuous disparity output.

In stereo, the general rule of thumb is that the disparity search range must be  $1/10$  the image size. In the new algorithm, BRAM usage scales linearly with disparity search range and scales again linearly with line width. So a doubling of image size, say from 640 to 1,280,

would in the previous design be an effective  $4\times$  of BRAM usage:  $2\times$  for line width,  $2\times$  again for disparity search range.

The minimum strip size is twice the search range, and will produce an output strip width equal to the disparity search range. So assuming a disparity search range of  $1/10$  image width, 10 sequential runs of the minimum strip size would produce a full output image.

This approach allowed the innovators to fit  $1280\times 960$  wide SAD5 stereo disparity

in less than 80 BRAM, 52k Slices on a Virtex 5LX330T, 25% and 24% of resources, respectively. Using a 100-MHz clock, this build would perform stereo at 39 Hz.

Of particular interest to JPL is that there is a flight qualified version of the Virtex 5: this could produce stereo results even for very large image sizes at 3 orders of magnitude faster than could

be computed on the PowerPC 750 flight computer. The work covered in the report allows the stereo algorithm to run on much larger images than before, and using much less BRAM. This opens up choices for a smaller flight FPGA (which saves power and space), or for other algorithms in addition to SAD5 to be run on the same FPGA.

*This work was done by Carlos Y. Villalpando and Arin C. Morfopoulos of Caltech for NASA's Jet Propulsion Laboratory. Further information is contained in a TSP (see page 1).*

*The software used in this innovation is available for commercial licensing. Please contact Daniel Broderick of the California Institute of Technology at [danielb@caltech.edu](mailto:danielb@caltech.edu). Refer to NPO-47245.*





## Hybrid Composite Cryogenic Tank Structure

**A number of materials can be used to produce external and internal layers of the structure.**

*Marshall Space Flight Center, Alabama*

A hybrid lightweight composite tank has been created using specially designed materials and manufacturing processes. The tank is produced by using a hybrid structure consisting of at least two reinforced composite material systems. The inner composite layer comprises a distinct fiber and resin matrix suitable for cryogenic use that is a braided-sleeve (and/or a filament-wound layer) aramid fiber preform that is placed on a removable mandrel (out-fitted with metallic end fittings) and is infused (vacuum-assisted resin transfer molded) with a polyurethane resin matrix with a high ductility at low temperatures. This inner layer is allowed to cure and is encapsulated with a filament-wound outer composite layer of a distinct fiber resin system. Both inner and outer layer are in intimate contact, and can also be cured at the same time. The

outer layer is a material that performs well for low temperature pressure vessels, and it can rely on the inner layer to act as a liner to contain the fluids.

The outer layer can be a variety of materials, but the best embodiment may be the use of a continuous tow of carbon fiber (T-1000 carbon, or others), or other high-strength fibers combined with a high ductility epoxy resin matrix, or a polyurethane matrix, which performs well at low temperatures. After curing, the mandrel can be removed from the outer layer.

While the hybrid structure is not limited to two particular materials, a preferred version of the tank has been demonstrated on an actual test tank article cycled at high pressures with liquid nitrogen and liquid hydrogen, and the best version is an inner layer of PBO (poly-phenylenebenzobisoxazole) fibers with a

polyurethane matrix and an outer layer of T-1000 carbon with a high elongation epoxy matrix suitable for cryogenic temperatures. A polyurethane matrix has also been used for the outer layer. The construction method is ideal because the fiber and resin of the inner layer has a high strain to failure at cryogenic temperatures, and will not crack or produce leaks. The outer layer serves as more of a high-performance structural unit for the inner layer, and can handle external environments.

*This work was done by Thomas DeLay of Marshall Space Flight Center.*

*This invention is owned by NASA, and a patent application has been filed. For further information, contact Sammy Nabors, MSFC Commercialization Assistance Lead, at [sammy.a.nabors@nasa.gov](mailto:sammy.a.nabors@nasa.gov). Refer to MFS-32390-1.*

## Nanoscale Deformable Optics

**This technology has potential applications in medical imaging, robotics, precision machining, and threat detection.**

*NASA's Jet Propulsion Laboratory, Pasadena, California*

Several missions and instruments in the conceptual design phase rely on the technique of interferometry to create detectable fringe patterns. The intimate emplacement of reflective material upon electron device cells based upon chalcogenide material technology permits high-speed, predictable deformation of the reflective surface to a sub-nanometer or finer resolution with a very high degree of accuracy.

In this innovation, a layer of reflective material is deposited upon a wafer containing (perhaps in the millions) chalcogenic memory cells with the reflective material becoming the front surface of a mirror and the chalcogenic material becoming a means of selectively deforming the mirror by the application of heat to the chalcogenic material. By doing so, the mirror surface can

deform anywhere from nil to nanometers in spots the size of a modern day memory cell, thereby permitting real-time tuning of mirror focus and reflectivity to mitigate aberrations caused elsewhere in the optical system.

Modern foundry methods permit the design and manufacture of individual memory cells having an area of or equal to the Feature (F) size of the design (assume 65 nm). Fabrication rules and restraints generally require the instantiation of one memory cell to another no closer than 1.5 F, or, for this innovation, 90 nm from its neighbor in any direction.

Chalcogenide is a semiconducting glass compound consisting of a combination of chalcogen ions, the ratios of which vary according to properties desired. It has been shown that the applica-

tion of heat to cells of chalcogenic material cause a large alteration in resistance to the range of 4 orders of magnitude. It is this effect upon which chalcogenide-based commercial memories rely. Upon removal of the heat source, the chalcogenide rapidly cools and remains frozen in the excited state. It has also been shown that the chalcogenide expands in volume because of the applied heat, meaning that the coefficient of expansion of chalcogenic materials is larger than 1.

In this innovation, chalcogenide-based cells are addressed (as though they are a memory), and heated and cooled according to well-established criteria. In doing so, the exact size of chalcogenide cell deformation is known and predictable; therefore, the deformation of the reflective surface is, likewise,

known and predictable. Control electronics can also be implemented so that a closed-loop feedback can be maintained. Changing the contents of the chalcogenide memory cells can compen-

sate for any change in environmental effects that might cause a change in optical path. This real-time control provides significant control and stability in use conditions.

*This work was done by Karl F. Strauss and Douglas J. Sheldon of Caltech for NASA's Jet Propulsion Laboratory. For more information, contact iaoffice@jpl.nasa.gov. NPO-46891*

---

## **Reliability-Based Design Optimization of a Composite Airframe Component**

**This methodology accommodates uncertainties in load, strength, and material properties.**

*John H. Glenn Research Center, Cleveland, Ohio*

A stochastic optimization methodology (SDO) has been developed to design airframe structural components made of metallic and composite materials. The design method accommodates uncertainties in load, strength, and material properties that are defined by distribution functions with mean values and standard deviations. A response parameter, like a failure mode, has become a function of reliability. The primitive variables like thermomechanical loads, material properties, and failure theories, as well as variables like depth of beam or thickness of a membrane, are considered random parameters with specified distribution functions defined by mean values and standard deviations.

The cumulative distribution concept is used to estimate the value of the response parameter like stress, displace-

ment, and frequency for a specified reliability. This solution for stochastic optimization also yields the design and weight of a structure as a function of reliability. Weight versus reliability is traced out in an inverted S-shaped graph. The center of the graph corresponds to 50-percent probability of success, or one failure in two samples.

A heavy design with weight approaching infinity could be produced for a near-zero rate of failure. Likewise, weight can be reduced to a small value for the most failure-prone design. Reliability can be changed for different components of an airframe structure. For example, the landing gear of an airliner can be designed for very high reliability, whereas it can be reduced for a raked wingtip.

The design capability is obtained by combining three codes: MSC/Nastran

code (the deterministic analysis tool), the fast probabilistic integration or the FPI module of the NESSUS software (the probabilistic calculator), and NASA Glenn's optimization testbed CometBoards (the optimizer). For the raked wingtip structure of the Boeing 767-400ER airliner, the stochastic optimization process redistributed the strain field and reduced weight by 17 percent over the traditional design.

*This work was done by Shantaram S. Pai and Rula Coroneos of Glenn Research Center and Surya N. Patnaik of Ohio Aerospace Institute. Further information is contained in a TSP (see page 1).*

*Inquiries concerning rights for the commercial use of this invention should be addressed to NASA Glenn Research Center, Innovative Partnerships Office, Attn: Steve Fedor, Mail Stop 4-8, 21000 Brookpark Road, Cleveland, Ohio 44135. Refer to LEW-18497-1.*

---

## **Zinc Oxide Nanowire Interphase for Enhanced Lightweight Polymer Fiber Composites**

**This technique can be used in applications requiring reduced structural mass, such as in aircraft, missiles, rockets, and balloons.**

*NASA's Jet Propulsion Laboratory, Pasadena, California*

The objective of this work was to increase the interfacial strength between aramid fiber and epoxy matrix. This was achieved by functionalizing the aramid fiber followed by growth of a layer of ZnO nanowires on the fiber surface such that when embedded into the polymer, the load transfer and bonding area could be substantially enhanced. The functionalization procedure developed here created functional carboxylic acid surface groups that chemically interact with the ZnO and thus greatly enhance the strength of the interface between the fiber and the ZnO.

The matrix-ZnO interface is enhanced through increased surface area (>1,000 times), mechanical interlocking, and the creation of a functional gradient between the nanowires and matrix, which has been shown to improve the interface strength of a carbon fiber composite by well over 100 percent. The composite compressive strength, shear strength, shear modulus, interlaminar shear strength, and interfacial shear strength should all be enhanced because the graded interface reduces the stress concentration at the discrete fiber-to-matrix boundary.

The first milestone of the project was to develop the functionalization procedure to enhance the attachment of the ZnO nanowires to the aramid fiber. This was achieved with carboxylic acid groups that split the peptide bond, catalyzed by a strong base, and created a carboxylate and a primary amine functional group. Carboxylic acid groups are specifically chosen because they often discharge a proton leading to charge coordination between the negative oxygen atoms and the positive zinc ions. Furthermore, the bond angles of carboxylic acid functional groups are



highly compatible with the zinc ion, making it the ideal functional group for bonding with zinc. Fourier Transform Infrared Spectroscopy (FTIR) was used for analyzing the absorbance frequencies and comparing to previously reported values, reactions, and bond structures for validation.

Single-fiber mechanical testing helped to determine the fiber tensile strength of the ZnO nanowire arrays. The results of the testing showed that

there was no degradation of the fiber strength in spite of breaking enough surface bonds to create functional groups onto which to anchor the nanowires. It is critical that fiber strength is maintained during functionalization and growth, because the composite properties depend heavily on that fiber strength. Composite lamina mechanical testing was also employed. Because ZnO nanowire arrays have been shown to increase interfacial shear strength at the

single fiber scale, improvements are expected in several properties at the composite scale. Interlaminar shear strength, laminar shear strength, and laminar shear modulus are expected to increase as a direct result of the functional gradient.

*This work was done by Henry A. Sodano of Arizona State University and Robert Brett Williams of Raytheon for NASA's Jet Propulsion Laboratory. For more information, contact [iaoffice@jpl.nasa.gov](mailto:iaoffice@jpl.nasa.gov). NPO-47214*





### ⚙️ Plasma Igniter for Reliable Ignition of Combustion in Rocket Engines

*Marshall Space Flight Center, Alabama*

A plasma igniter has been developed for initiating combustion in liquid-propellant rocket engines. The device propels a hot, dense plasma jet, consisting of elemental fluorine and fluorine compounds, into the combustion chamber to ignite the cold propellant mixture. The igniter consists of two coaxial, cylindrical electrodes with a cylindrical bar of solid Teflon plastic in the region between them. The outer electrode is a metal (stainless steel) tube; the inner electrode is a metal pin (mild steel, stainless steel, tungsten, or thoriated-tungsten). The Teflon bar fits snugly between the two electrodes and provides electrical insulation between them. The Teflon bar may have either a

flat surface, or a concave, conical surface at the open, down-stream end of the igniter (the igniter face). The igniter would be mounted on the combustion chamber of the rocket engine, either on the injector-plate at the upstream side of the engine, or on the sidewalls of the chamber. It also might sit behind a valve that would be opened just prior to ignition, and closed just after, in order to prevent the Teflon from melting due to heating from the combustion chamber.

The plasma jet deposits the energy required to initiate combustion, while highly reactive fluorine and fluorine compounds create free-radicals in the flow-field to further promote rapid igni-

tion. The plasma jet is created and accelerated electrically, and the feedstock for the plasma is maintained in a solid, inert form, leading to a rugged, reliable and compact design. The device should promote rapid and reliable ignition in LOX/LCH<sub>4</sub> engines in particular, and in liquid propellant engines in general. It could also be used in gas-turbine engines where prompt and reliable restart is critically important; for example, in helicopter and jet aircraft engines.

*This work was done by Adam Martin and Richard Eskridge of Marshall Space Flight Center. For further information, contact Sammy Nabors, MSFC Commercialization Assistance Lead, at [sammy.a.nabors@nasa.gov](mailto:sammy.a.nabors@nasa.gov). Refer to MFS-32557-1.*

### ⚙️ Wire Test Grip Fixture

**This fixture can be used in any thin-gauge wire testing.**

*John H. Glenn Research Center, Cleveland, Ohio*

Wire-testing issues, such as the gripping strains imposed on the wire, play a critical role in obtaining clean data. In a standard test frame fitted with flat wedge grips, the gripping action alone creates stresses on the wire specimen that cause the wire to fail at the grip location. When conventional wire grip fixtures are installed, the test span as well as the amount of wire used increase dramatically due to the large nature of the wire testing fixture. A new test frame, which is outfitted with a vacuum chamber, negated the use of any conventional commercially available wire test fixtures, as only 7 in. (17.8 cm) existed between the grip faces.

An innovative grip fixture was designed to test thin gauge wire for a variety of applications in an existing Instron test frame outfitted with a vacuum chamber. This unit was designed to adapt to a predetermined test span constrained by the vacuum chamber. The test frame was fitted with flat grips so that no gripping strain was induced into the brittle wire specimen.

In order to accomplish the task of testing small-diameter brittle wire, a very simple test fixture was designed. The first task was to create a technique to relieve the strains induced into the wire upon gripping. This was accomplished with two 1.5 in. (38 mm) wire spools. These spools were designed to relieve the gripping strains by wrapping the wire around the spools to grip the fixtures circumferentially. On each spool, a small bolt was installed to attach the wire to the spool. These bolts were placed 270° around the diameter of the spool so the wire contacted around the wheel. The concept employed ensured that the strains in the wire due to gripping would be reduced by the smooth transition around the wheel. A small groove was machined into the spools to center the wire.

In an effort to save test wire, as well as simplify the installation of the test wire to the spools, a locating rail was devised. This rail established the span of the gripping spools by pinning the spools to a thin, flat plate. When assembled, the

wire is easily wrapped around and secured to the spools. The wire is pre-loaded slightly on the fixture to stay in place. This unit is then installed into the test frame. The leading edge of the rail was designed to match up to the grips installed in the test frame.

The machine was placed in the test-ready position. The loaded test rail was installed up against the sides of the flat test wedge grips, which, by design, established the test wire centered in the test frame. Pre-existing marks on the test spools allow the operator to center the fixture, top to bottom, prior to gripping. The test spools were machined to a width of 0.025 in. (0.64 mm), matching that of a standard, flat test specimen. When the flat wedge grips were closed, the wedges gripped the spools and established the test span. After the grips seat, the test rail can be removed, and the wire is ready to test. If for some reason the specimen needs to be removed from the test frame, the installation rail can be reinstalled on the pinned spools and

the sample ungripped. This design uses about 8-in. (20-cm) of wire per tests. Multiple tests were conducted at both room and elevated temperature with no failures in the grip region.

The novelty of this wire test fixture lies in its simplicity. Its compact features allow the user to install the fixture in a test frame with little or no modifica-

tions. The self-alignment feature designed into set-up places the wire specimen in perfect alignment with the test frame. The loading spools, when gripped, are in direct contact with the test frame water-cooled wedge grips. This helps to draw temperature away from the fixture for ease of high-temperature testing.

*This work was done by Christopher S. Burke of Glenn Research Center. Further information is contained in a TSP (see page 1).*

*Inquiries concerning rights for the commercial use of this invention should be addressed to NASA Glenn Research Center, Innovative Partnerships Office, Attn: Steven Fedor, Mail Stop 4-8, 21000 Brookpark Road, Cleveland, Ohio 44135. Refer to LEW-18579-1.*

## ⚙️ A Sub-Hertz, Low-Frequency Vibration Isolation Platform

**This system can be used for vibration isolation in semiconductor manufacturing, for space-based imaging systems, or fine pointing of free-space optical communication transceivers.**

*NASA's Jet Propulsion Laboratory, Pasadena, California*

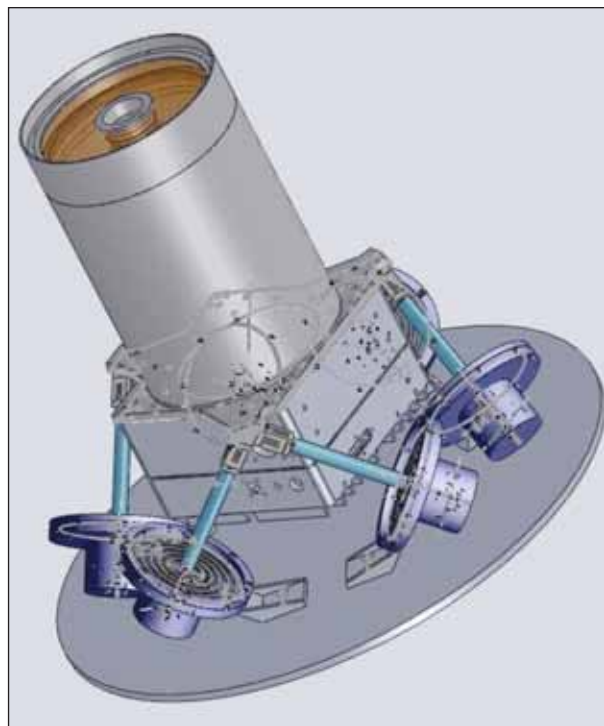
One of the major technical problems deep-space optical communication (DSOC) systems need to solve is the isolation of the optical terminal from vibrations produced by the spacecraft navigational control system and by the moving parts of onboard instruments. Even under these vibration perturbations, the DSOC transceivers (telescopes) need to be pointed 1000's of times more accurately than an RF communication system (parabolic antennas).

Mechanical resonators have been extensively used to provide vibration isolation for ground-based, airborne, and spaceborne payloads. The effectiveness of these isolation systems is determined mainly by the ability of designing a mechanical oscillator with the lowest possible resonant frequency. The Low-Frequency Vibration Isolation Platform (LFVIP), developed during this effort, aims to reduce the resonant frequency of the mechanical oscillators into the sub-Hertz region in order to maximize the passive isolation afforded by the 40 dB/decade roll-off response of the resonator. The LFIIP also provides tip/tilt functionality for acquisition and tracking of a beacon signal. An active control system is used for platform positioning and for dampening of the mechanical oscillator.

The basic idea in the design of the isolation platform is to use a passive isolation strut with a  $\approx 100$ -mHz resonance frequency. This will extend the isolation

range to lower frequencies. The harmonic oscillator is a second-order low-pass filter for mechanical disturbances. The resonance quality depends on the dissipation mechanisms, which are mainly hysteretic because of the low resonant frequency and the absence of any viscous medium.

The LFIIP system is configured using the well-established Stewart Platform, which consists of a top platform connected to a base with six extensible struts



A CAD rendering of the Low-Frequency Vibration Isolation Platform with payload. Shown is the configuration of the six LFIIP struts (four shown). One of the lower left struts clearly shows the steel membrane with its topology designed to have a reasonably high stiffness along the membrane plane.

(see figure). The struts are attached to the base and to the platform via universal joints, which permit the extension and contraction of the struts. The struts' ends are connected in pairs to the base and to the platform, forming an octahedron. The six struts provide the vibration isolation due to the properties of mechanical oscillators that behave as second-order low-pass filters for frequencies above the resonance. At high frequency, the ideal second-order low-pass filter response is spoiled by the distributed mass and the internal modes of membrane and of the platform with its payload.

The mechanical oscillator is implemented using a particular geometry of a stainless steel membrane. This geometry provides a very soft mechanical compliance along the axis orthogonal to the membrane and about axes coplanar to the membrane. It also allows the design of a membrane with sufficiently stiff compliances on the other remaining directions.

The proposed LFIIP has the potential to yield a low-power, low-mass isolation system for payloads requiring stable platforms, such as imaging and free-space optical communications.

*This work was done by Gerardo G. Ortiz, William H. Farr, and Virginio Sannibale of Caltech for NASA's Jet Propulsion Laboratory. For more information, contact [iaoffice@jpl.nasa.gov](mailto:iaoffice@jpl.nasa.gov). NPO-46862*



## Carbon Nanofibers Synthesized on Selective Substrates for Nonvolatile Memory and 3D Electronics

This method can impact the application of carbon nanofiber tubes in 3D electronics applications.

NASA's Jet Propulsion Laboratory, Pasadena, California

A plasma-enhanced chemical vapor deposition (PECVD) growth technique has been developed where the choice of starting substrate was found to influence the electrical characteristics of the resulting carbon nanofiber (CNF) tubes. It has been determined that, if the tubes are grown on refractory metallic nitride substrates, then the resulting tubes formed with dc PECVD are also electrically conducting.

Individual CNFs were formed by first patterning Ni catalyst islands using e-beam evaporation and liftoff. The CNFs were then synthesized using dc PECVD with  $C_2H_2:NH_3 = [1:4]$  at 5 Torr and 700 °C, and  $\approx 200$ -W plasma power. Tubes were grown directly on degenerately doped silicon  $\langle 100 \rangle$  substrates with resistivity  $\rho \approx 1\text{--}5 \text{ m}\Omega\text{-cm}$ , as well as NbTiN. The  $\approx 200$ -nm thick refractory NbTiN deposited using magnetron sputtering had  $\rho \approx 113 \mu\Omega\text{-cm}$  and was also chemically compatible with CNF synthesis. The sample was then mounted on a 45° beveled Al holder, and placed inside a SEM (scanning electron microscope). A nanomanipulator probe stage was placed inside the SEM equipped with an electrical feed-through, where tungsten probes were used to make two-terminal electrical measurements with an HP 4156C parameter analyzer.

The positive terminal nanoprobe was mechanically manipulated to physically contact an individual CNF grown on NbTiN as shown by the SEM image in the inset of figure (a), while the negative terminal was grounded to the substrate. This revealed the tube was electrically conductive, although measurable currents could not be detected until  $\approx 6 \text{ V}$ , after which point current increased sharply until compliance ( $\approx 50 \text{ nA}$ ) was reached at  $\approx 9.5 \text{ V}$ . A native oxide on the tungsten probe tips may contribute to a tunnel barrier, which could be the reason for the suppressed transport at low biases. Currents up to  $\approx 100 \text{ nA}$  could be cycled, which are likely to propagate via the

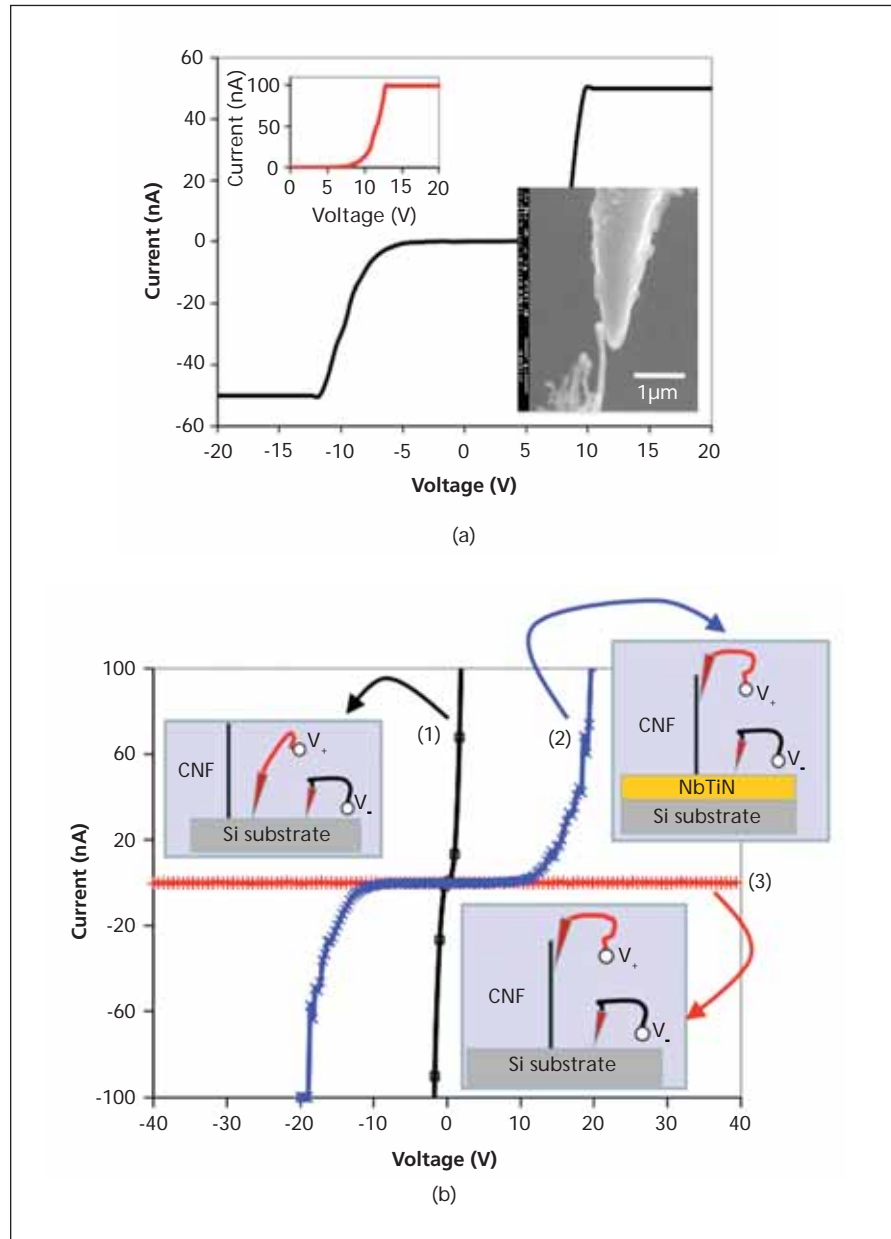


Figure (a) Electrical Transport Measurements for a single CNF grown on an NbTiN buffer layer on Si. A nanoprobe was in contact with a CNF, as the SEM image in the inset indicates. The top inset shows the I-V characteristic when compliance was increased to 100 nA. (b) Curve (1) corresponds to the case where both probes were shorted to the substrate and indicates high conductivity; curve (2) shows the CNF grown on NbTiN was electrically conductive; curve (3) corresponds to the case where no electrical conduction was detected for a CNF grown directly on Si, and suggests such CNFs are unsuitable for dc NEMS applications.

tube surface, or sidewalls, rather than the body, which is shown by the I-V in figure (a).

Electrical conduction via the sidewalls is a necessity for dc NEMS (nanoelectromechanical system) applications, more so than for the field emission applications of such tubes. During the tests, high conductivity was expected, because both probes were shorted to the substrate, as shown by curve 1 in the I-V characteristic in figure (b). When a tube grown on NbTiN was probed, the response was similar to the  $\approx 100$  nA and is represented by

curve 2 in figure (b), which could be cycled and propagated via the tube surface or the sidewalls. However, no measurable currents for the tube grown directly on Si were observed as shown by curve 3 in figure (b), even after testing over a range of samples. This could arise from a dielectric coating on the sidewalls for tubes on Si. As a result of the directional nature of ion bombardment during dc PECVD, Si from the substrate is likely re-sputtered and possibly coats the sidewalls.

*This work was done by Anupama B. Kaul and Abdur R. Khan of Caltech for NASA's Jet*

*Propulsion Laboratory. For more information, contact [iaoffice@jpl.nasa.gov](mailto:iaoffice@jpl.nasa.gov).*

*In accordance with Public Law 96-517, the contractor has elected to retain title to this invention. Inquiries concerning rights for its commercial use should be addressed to:*

*Innovative Technology Assets Management  
JPL*

*Mail Stop 202-233*

*4800 Oak Grove Drive*

*Pasadena, CA 91109-8099*

*E-mail: [iaoffice@jpl.nasa.gov](mailto:iaoffice@jpl.nasa.gov)*

*Refer to NPO-47157, volume and number of this NASA Tech Briefs issue, and the page number.*

---

## Nanoparticle/Polymer Nanocomposite Bond Coat or Coating

*John H. Glenn Research Center, Cleveland, Ohio*

This innovation addresses the problem of coatings (meant to reduce gas permeation) applied to polymer matrix composites spalling off in service due to incompatibility with the polymer matrix. A bond coat/coating has been created that uses chemically functionalized nanoparticles (either clay or graphene) to create a barrier film that bonds well to the matrix resin, and provides an outstanding barrier to gas permeation.

There is interest in applying clay nanoparticles as a coating/bond coat to a polymer matrix composite. Often, nanoclays are chemically functionalized with

an organic compound intended to facilitate dispersion of the clay in a matrix. That organic modifier generally degrades at the processing temperature of many high-temperature polymers, rendering the clay useless as a nano-additive to high-temperature polymers. However, this innovation includes the use of organic compounds compatible with high-temperature polymer matrix, and is suitable for nanoclay functionalization, the preparation of that clay into a coating/bondcoat for high-temperature polymers, the use of the clay as a coating for composites that do not have a high-

temperature requirement, and a comparable approach to the preparation of graphene coatings/bond coats for polymer matrix composites.

*This work was done by Sandi G. Miller of Glenn Research Center. Further information is contained in a TSP (see page 1).*

*Inquiries concerning rights for the commercial use of this invention should be addressed to NASA Glenn Research Center, Innovative Partnerships Office, Attn: Steven Fedor, Mail Stop 4-8, 21000 Brookpark Road, Cleveland, Ohio 44135. Refer to LEW-18607-1.*



### **High-Resolution Wind Measurements for Offshore Wind Energy Development**

*NASA's Jet Propulsion Laboratory, Pasadena, California*

A mathematical transform, called the Rosette Transform, together with a new method, called the Dense Sampling Method, have been developed. The Rosette Transform is invented to apply to both the mean part and the fluctuating part of a targeted radar signature using the Dense Sampling Method to construct the data in a high-resolution grid at 1-km posting for wind measurements over water surfaces such as oceans or lakes.

This new technique enables the use of NASA satellite scatterometer data, such as QuikSCAT data, which have been collected globally over a decade for measur-

ing high-resolution wind field at 1-km posting on water surfaces. Valid in near-shore waters (10–15 km from shore), the high-resolution wind data are unique and critical to calculate accurate wind power density and its variability for the development of future offshore wind farms. The new technique was originally developed to monitor urban and suburban environments, and it has been applied to obtain high-resolution radar signatures over ocean and lake environments for high-resolution wind measurements.

*This work was done by Son V. Nghiem and Gregory Neumann of Caltech for NASA's Jet*

*Propulsion Laboratory. For more information, contact [iaoffice@jpl.nasa.gov](mailto:iaoffice@jpl.nasa.gov).*

*In accordance with Public Law 96-517, the contractor has elected to retain title to this invention. Inquiries concerning rights for its commercial use should be addressed to:*

*Innovative Technology Assets Management  
JPL*

*Mail Stop 202-233  
4800 Oak Grove Drive  
Pasadena, CA 91109-8099*

*E-mail: [iaoffice@jpl.nasa.gov](mailto:iaoffice@jpl.nasa.gov)*

*Refer to NPO-46909, volume and number of this NASA Tech Briefs issue, and the page number.*

### **Spring Tire**

**This tire design can be used where low vehicle energy consumption is required and for vehicles traveling over rough terrain.**

*John H. Glenn Research Center, Cleveland, Ohio*

The spring tire is made from helical springs, requires no air or rubber, and consumes nearly zero energy. The tire design provides greater traction in sandy and/or rocky soil, can operate in micro-gravity and under harsh conditions (vastly varying temperatures), and is non-pneumatic.

Like any tire, the spring tire is approximately a toroidal-shaped object intended to be mounted on a transportation wheel. Its basic function is also similar to a traditional tire, in that the spring tire contours to the surface on which it is driven to facilitate traction, and to reduce the transmission of vibration to the vehicle. The essential difference between other tires and the spring tire is the use of helical springs to support and/or distribute load. They are coiled wires that deform elastically under load with little energy loss.

This design is an advancement of the wire-mesh tire technology defined under U.S. Patent 3,568,748, entitled "Resilient Wheel." The difference between the two tire technologies is the



The **Spring Tire**, co-invented by NASA Glenn Research Center and the Goodyear Tire & Rubber Company. This airless, rubberless tire is capable of contouring to the rocky surface of the Moon, yet consumes far less energy than an Earth tire. Photo Credit — Aaron Vandersomers/Goodyear

fundamental element used to create the wire mesh that forms the tire. The resilient wheel uses crimped wire mesh to form the tire, but the spring tire uses a coiled wire mesh. Under the weight of the vehicle, the tire is driven or towed, as well as steered. The springs within the tire passively contour to the terrain by flexing and moving with respect to each other.

There are three steps required to manufacture the spring tire. First, the springs are twisted together to form a rectangular sheet with length of the tire circumference. Second, the ends of the rectangular sheet of springs are interlaced to form a mesh cylinder. Third, one end of the mesh cylinder is collapsed and attached to the wheel, and the other end is flipped inside out, attaching it to the opposite end of the wheel.

The load-support springs are configured radially. This mitigates the pantographing of springs (rotation at their intersections). As a result, a relatively high mesh density may be used without excessive interference and stress be-

tween neighboring springs. Elimination of pantographing also reduces friction forces.

The load support springs are also interwoven. This minimizes or eliminates the need for load distribution springs to hold the load support springs together. With fewer load distribution springs, the load support springs con-

tour more freely and the overall tire weight is reduced. Cross-sections of the tire are approximately round, which distributes applied loads relatively uniformly. This reduces tire stresses and improves flotation and traction development in soft soil.

*This work was done by Vivake M. Asnani of Glenn Research Center and Jim Benzing and*

*Jim C. Kish of Goodyear Tire & Rubber Company. Further information is contained in a TSP (see page 1).*

*Inquiries concerning rights for the commercial use of this invention should be addressed to NASA Glenn Research Center, Innovative Partnerships Office, Attn: Steve Fedor, Mail Stop 4-8, 21000 Brookpark Road, Cleveland, Ohio 44135. Refer to LEW-18466-1.*





## Marsviewer 2008

Marsviewer 2008 is designed for quality control, browsing, and operational and science analysis of images and derived image products returned by spacecraft. This program allows all derived products (reduced data records, or RDRs) associated with each original image (experiment data record, or EDR) to be viewed in various ways, including in stereo, depending on the type of image.

The program features a pluggable interface called a “file finder.” This encapsulates knowledge of a specific mission’s filename and directory conventions, hiding the complexity behind each mission from the user, and allowing new missions to be added easily. Within a mission, different directory conventions can also be supported. This file-finder interface presents a similar interface to the user for all these missions and directory structures. All EDRs found for a given Sol are displayed in a list (optionally with thumbnail images) for the user to pick from.

Once an image is picked, a primary (vertical) tab pane allows the user to select the left or right image, left or right thumbnail, or stereo views. A secondary (horizontal) tab pane allows the EDR, or any of its RDRs, to be viewed. Most RDRs may be viewed independently, or as colored overlays on a background image. Each of the 41 RDR types has a display method appropriate for that type, and most have display parameters that can be adjusted.

The program understands two different image geometries (raw and linearized), and can show the actual pixel values under the cursor for every EDR and RDR matching the geometry type at once. Various display manipulations, such as zoom, data range, contrast enhancement, interval selection, and contour controls are available. Metadata (image labels) may be displayed and searched as well. The stereo display shows both left and right images simultaneously. It works either in anaglyph mode (red/blue glasses), or by using dedicated display hardware.

This innovation also covers the applications “jadeviewer” and “jade\_overlay,” which are closely related derivatives from Marsviewer. The “jadeviewer”

application reuses the image display and visualization portions of Marsviewer without the file finder. The user directly specifies filenames and RDR type, and can then view the product as with Marsviewer.

*This work was done by Nicholas T. Toole and Robert G. Deen of Caltech for NASA’s Jet Propulsion Laboratory. For more information, contact [iaoffice@jpl.nasa.gov](mailto:iaoffice@jpl.nasa.gov).*

*The software used in this innovation is available for commercial licensing. Please contact Daniel Broderick of the California Institute of Technology at [danielb@caltech.edu](mailto:danielb@caltech.edu). Refer to NPO-46698.*

## Mission Services Evolution Center Message Bus

The Goddard Mission Services Evolution Center (GMSEC) Message Bus is a robust, lightweight, fault-tolerant middleware implementation that supports all messaging capabilities of the GMSEC API, including publish/subscribe and request/reply. The Message Bus enables NASA to provide an open-source middleware solution, for no additional cost, that is self-configuring, easy to install, and can be used for the development of GMSEC-compliant components. Some professional capabilities provided by this software include failover and fault tolerance, good performance, compression, debugging, and wide platform support.

This architecture is a distributed software system that routes messages based on message subject names and knowledge of the locations in the network of the interested software components. Functional software components register with the message bus, so that a location directory can be maintained. The functional applications then send messages onto the bus with an indication of the message type/subject/etc. Other applications that want to receive data register with the message bus and indicate what message types/subjects they want to receive. The message bus maintains a routing table where routes publish messages to the applications that have requested them. One message may be delivered to many different applications. Use of the message bus eliminates the need for each application to create separate communications paths with each application to which it interfaces.

The nature of the GMSEC Message Bus enables any project or user to quickly take the initial steps for creating or connecting GMSEC-compliant components, and for developing small systems without high license fees and learning curves. This software uses middleware to facilitate cross application or component communication on a software bus.

*This work was done by Arturo Mayorga and John O. Bristow of Goddard Space Flight Center and Mike Butschky of Interface and Control Systems. Further information is contained in a TSP (see page 1). GSC-15575-1*

## Major Constituents Analysis for the Vehicle Cabin Atmosphere Monitor

Vehicle Cabin Atmosphere Monitor (VCAM) can provide a means for monitoring the air within enclosed environments such as the International Space Station, the Crew Exploration Vehicle (CEV), a Lunar habitat, or another vehicle traveling to Mars. Its miniature pre-concentrator, gas chromatograph (GC), and mass spectrometer can provide unbiased detection of a large number of organic species. VCAM’s software can identify whether the chemicals are on a targeted list of hazardous compounds and their concentration. Its performance and reliability on orbit, along with the ground team’s assessment of its raw data and analysis results, will validate its technology for future use and development.

The software processes a sum total spectra (counts vs. mass channel) with the intention of computing abundance ratios for N<sub>2</sub>, O<sub>2</sub>, CO<sub>2</sub>, Ar<sub>2</sub>, and H<sub>2</sub>O. A brute-force powerset expansion compares a library of expected mass lines with those found within the data. Least squares error is combined with a penalty term for using small peaks. This permits calibration even in the presence of unexpected/unknown system contamination or unknown/novel ratios of atmospheric constituents.

Automated, reliable mass calibration is a substantial improvement beyond other comparable systems. A method of compensation for variable response component spectra has been utilized via a weighted sum based on the central peak for each expected component.

It is fully autonomous, non-GUI-based, self-calibrating, and compliant with the VWORKS flight software system.

*This work was done by Lukas Mandrake, Benjamin J. Bornstein, Stojan Madzunkov, and John A. Macaskill of Caltech for NASA's Jet Propulsion Laboratory. For more information, contact [iaoffice@jpl.nasa.gov](mailto:iaoffice@jpl.nasa.gov).*

*The software used in this innovation is available for commercial licensing. Please contact Daniel Broderick of the California Institute of Technology at [danielb@caltech.edu](mailto:danielb@caltech.edu). Refer to NPO-46956.*

## Astronaut Health Participant Summary Application

The Longitudinal Study of Astronaut Health (LSAH) Participant Summary software captures data based on a custom information model designed to gather all relevant, discrete medical events for its study participants. This software provides a summarized view of the study participant's entire medical record. The manual collapsing of all the data in a participant's medical record into a summarized form eliminates redundancy, and allows for the capture of entire medical events. The coding tool could be incorporated into commercial electronic medical record software for use in areas like public health surveillance, hospital systems, clinics, and medical research programs.

The software also enables structured coding that enforces a custom set of rules, as well as captures the context of the coded term. The terminology used is SNOMED CT, which is a massive terminology consisting of over 366,000 concepts with unique meanings and formal, logic-based definitions that are organized into 18 hierarchies. In addition, it contains more than 993,000 descriptions or synonyms for flexibility in expressing clinical concepts. SNOMED CT is also a compositional terminology, so multiple concepts can be grouped together to create an expression that has a totally different logical definition. By using some custom composition rules along with the context within the Participant Summary, a user can greatly reduce the number of candidate concepts, which not only improves productivity, it ensures that only legal SNOMED expressions can be created.

LSAH defines the line between the terminology and the information model. It takes a middle road between putting all the structure in a complex coded term and putting all the structure in numerous database fields.

*This work was done by Kathy Johnson-Throop of Johnson Space Center; Ralph Krog of National Space Biomedical Research Institute; Deborah Eudy and Diane Parisian of EASI; Seth Rodriguez and John Rogers of Barrios Technology; and Mary Wear, Robert Volpe, and Gina Trevino of Wyle Laboratories. Further information is contained in a TSP (see page 1). MSC-24172-1*

## Adaptation of the AMDIS Method to Flight Status on the VCAM Instrument

Software has been developed to function onboard the International Space Station (ISS) to help safeguard human health by detecting compounds of concern in the cabin atmosphere, both in identity and concentration. This software calibrates and processes a standard 2D dataset (mass spectrum versus time) output from a gas chromatogram/mass spectrometer by identifying temporal events, including the possibility for near simultaneous event overlap, reducing the mass spectra for each event and comparing to an arbitrary library of known compounds. The level of autonomy, adjustment of parameters for the VCAM devices' specific data characteristics, and adaptive mass resolution to ease requirement of precision mass calibration are three unique features of this design. The estimation of concentration is also a significant addition to the standard AMDIS (NIST) implementation. Solution filtration based on elution time, and an arbitration algorithm for similar matches, provide the user with a more succinct, single-valued estimate in comparison to algorithms designed to merely augment expert hand analysis.

*This work was done by Lukas Mandrake, Benjamin J. Bornstein, Seungwon Lee, and Brian D. Bue of Caltech for NASA's Jet Propulsion Laboratory. For more information, contact [iaoffice@jpl.nasa.gov](mailto:iaoffice@jpl.nasa.gov).*

*The software used in this innovation is available for commercial licensing. Please contact Daniel Broderick of the California Institute of Technology at [danielb@caltech.edu](mailto:danielb@caltech.edu). Refer to NPO-46563.*

## Natural Language Interface for Safety Certification of Safety-Critical Software

Model-based design and automated code generation are being used increasingly at NASA. The trend is to move beyond simulation and prototyping to actual flight code, particularly in the

guidance, navigation, and control domain. However, there are substantial obstacles to more widespread adoption of code generators in such safety-critical domains. Since code generators are typically not qualified, there is no guarantee that their output is correct, and consequently the generated code still needs to be fully tested and certified.

The AutoCert generator plug-in supports the certification of automatically generated code by formally verifying that the generated code is free of different safety violations, by constructing an independently verifiable certificate, and by explaining its analysis in a textual form suitable for code reviews. This enables missions to obtain assurance about the safety and reliability of the code without excessive manual effort. The key technical idea is to exploit the idiomatic nature of auto-generated code in order to automatically infer logical annotations that describe properties of the code. These allow the automatic formal verification of the safety properties without requiring access to the internals of the code generator. The approach is therefore independent of the particular generator used. The use of a combined generation/analysis tool can allow system engineers to concentrate on the modeling and design, rather than worrying about low-level software details. By providing tracing between code and verification artifacts, and customizable safety reports, the tool supports both certification and debugging. Although integrated with the code generator, AutoCert is functionally independent in the sense that it does not rely on the correctness of any generator components. The tool has two main benefits: (1) it helps catch bugs in autocoders, and (2) it helps with the certification process for the autogenerated code, thus mitigating the risk of using COTS autocoders that lack a trusted heritage.

The AutoCert technology also has a number of advantages over other approaches to formal verification. It can handle code with arbitrary loops, and can handle code generated from both continuous and discrete models. Moreover, the certification system based on annotation inference is more flexible and extensible than decentralized architectures where certification information is distributed throughout the code generator. Identifying the patterns that are used to infer the annotations is an iterative process, but by allowing tracing between VCs (verification conditions) and state-

ments of the auto-generated code, the tool lets missing annotations and, thus, missing patterns, to be pinpointed more easily. By raising the level of abstraction at which verification knowledge is expressed, one can concisely

capture many variations of the underlying code idioms. In particular, one can easily deal with optimizations that obscure low-level code structure.

*This program was written by Ewen Denney and Bernd Fischer of USRA/RIACS for Ames*

*Research Center. Further information is contained in a TSP (see page 1).*

*Inquiries concerning rights for the commercial use of this invention should be addressed to the Ames Technology Partnerships Division at (650) 604-5761. Refer to ARC-15990-1.*





### **Cryogenic Caging for Science Instrumentation**

*NASA's Jet Propulsion Laboratory, Pasadena, California*

A method has been developed for caging science instrumentation to protect from pyro-shock and EDL (entry, descent, and landing) acceleration damage. Caging can be achieved by immersing the instrument (or its critical parts) in a liquid and solidifying the liquid by cooling. After the launch shock and/or after the payload has landed, the solid is heated up and evaporated.

In the example of a sensitive  $x$ - $y$  seismometer, the volume is filled with CO<sub>2</sub> (at an elevated pressure), or other compatible liquid. Then the liquid is frozen and maintained at a temperature below -80 °C for the duration of the flight. The solid is then allowed to sublime through a valved port. Other uses include caging of drag-free elements of LISA (laser interferometer space antenna) spacecraft

and their progeny, caging instrumentation and avionics for penetrator missions, and caging of electronics to survive launch shock.

*This work was done by Konstantin Penanen and Talso C. Chui of Caltech for NASA's Jet Propulsion Laboratory. Further information is contained in a TSP (see page 1). NPO-46930*

### **Wide-Range Neutron Detector for Space Nuclear Applications**

*John H. Glenn Research Center, Cleveland, Ohio*

A digital, wide-range, neutron detection (WRND) system in a compact, VME form factor monitors neutron activity within the core of a nuclear reactor across the reactor's entire operating range, from 1.0 n/cm<sup>2</sup>/s up to 10<sup>10</sup> n/cm<sup>2</sup>/s. This allows for a reduction in the complexity of space-based nuclear instrumentation systems, as a single instrument can be used instead of requiring different instrumentation for each of the operation ranges of the reactor (start-up, ramp-up, and nominal power).

This instrument consists of one or more fission chamber detectors, an integrated electronics module, and inter-

connected cabling, all of which are adapted for the space environment from proven, terrestrial-based technology. WRND delivers logarithmic output signals to a host system, proportional to neutron flux and rate across the entire operating range of the reactor. The electronics module hardware and firmware are the basis of the innovation.

WRND is broadly compatible with many potential future applications (nuclear power, nuclear propulsion, etc.). Nothing in the initial design assumes a particular type of reactor, or whether it will be vehicle- or land-based. This innovation's ability to function over a wide

range of neutron fluxes ensures its development is not necessarily linked with any particular reactor type, and in no way limits future nuclear power implementation options, while still providing NASA with the needed functionality.

*This work was done by John F. Merk of Aurora Flight Sciences and Alberto Busto of Black River Technology for Glenn Research Center.*

*Inquiries concerning rights for the commercial use of this invention should be addressed to NASA Glenn Research Center, Innovative Partnerships Office, Attn: Steve Fedor, Mail Stop 4-8, 21000 Brookpark Road, Cleveland, Ohio 44135. LEW-18469-1*

### **In Situ Guided Wave Structural Health Monitoring System**

*John H. Glenn Research Center, Cleveland, Ohio*

Aircraft engine rotating equipment operates at high temperatures and stresses. Noninvasive inspection of microcracks in those components poses a challenge for nondestructive evaluation. A low-cost, low-profile, high-temperature ultrasonic guided wave sensor was developed that detects cracks *in situ*. The transducer design provides nondestructive evaluation of structures and materials.

A key feature of the sensor is that it withstands high temperatures and excites strong surface wave energy to in-

spect surface and subsurface cracks. The sol-gel bismuth titanate-based surface acoustic wave (SAW) sensor can generate efficient SAWs for crack inspection. The sensor is very thin (sub-millimeter) and can generate surface waves up to 540 °C. Finite element analysis of the SAW transducer design was performed to predict the sensor behavior, and experimental studies confirmed the results.

The sensor can be implemented on structures of various shapes. With a spray-coating process, the sensor can be

applied to the surface of large curvatures. It has minimal effect on airflow or rotating equipment imbalance, and provides good sensitivity.

*This work was done by George Zhao of Intelligent Automation, Inc. and Bernhard R. Tittmann of The Pennsylvania State University for Glenn Research Center.*

*Inquiries concerning rights for the commercial use of this invention should be addressed to NASA Glenn Research Center, Innovative Partnerships Office, Attn: Steve Fedor, Mail Stop 4-8, 21000 Brookpark Road, Cleveland, Ohio 44135. Refer to LEW-18447-1.*

---

## Multiplexed Energy Coupler for Rotating Equipment

*John H. Glenn Research Center, Cleveland, Ohio*

A multiplexing antenna assembly can efficiently couple AC signal/energy into, or out of, rotating equipment. The unit only passes AC energy while blocking DC energy. Concentric tubes that are sliced into multiple pieces are assembled together so that, when a piece from an outer tube aligns well with an inner tube piece, efficient energy coupling is achieved through a capacitive scheme.

With  $N$  outer pieces and  $M$  inner pieces, an effective  $N \times M$  combination can be achieved in a multiplexed manner. The energy coupler is non-contact, which is useful if isolation from rotating and stationary parts is required. Additionally, the innovation can operate in high temperatures. Applications include rotating structure sensing, non-contact energy transmission, etc.

*This work was done by Xiaoliang Zhao of Intelligent Automation, Inc. for Glenn Research Center.*

*Inquiries concerning rights for the commercial use of this invention should be addressed to NASA Glenn Research Center, Innovative Partnerships Office, Attn: Steve Fedor, Mail Stop 4-8, 21000 Brookpark Road, Cleveland, Ohio 44135. Refer to LEW-18467-1*

---

## Attitude Estimation in Fractionated Spacecraft Cluster Systems

*NASA's Jet Propulsion Laboratory, Pasadena, California*

An attitude estimation was examined in fractionated free-flying spacecraft. Instead of a single, monolithic spacecraft, a fractionated free-flying spacecraft uses multiple spacecraft modules. These modules are connected only through wireless communication links and, potentially, wireless power links. The key advantage of this concept is the ability to respond to uncertainty. For example, if a single spacecraft module in the cluster fails, a new one can be launched at a lower cost and risk than would be incurred with on-orbit servicing or replacement of the monolithic spacecraft.

In order to create such a system, however, it is essential to know what the navigation capabilities of the fractionated system are as a function of the capabilities of the individual modules, and to have an algorithm that can perform estimation of the attitudes and relative positions of the modules with fractionated sensing capabilities.

Looking specifically at fractionated attitude estimation with startrackers and optical relative attitude sensors, a set of mathematical tools has been developed that specify the set of sensors necessary to ensure that the attitude of the entire cluster ("cluster attitude") can be ob-

served. Also developed was a navigation filter that can estimate the cluster attitude if these conditions are satisfied.

Each module in the cluster may have either a startracker, a relative attitude sensor, or both. An extended Kalman filter can be used to estimate the attitude of all modules. A range of estimation performances can be achieved depending on the sensors used and the topology of the sensing network.

*This work was done by Fred Y. Hadaegh and Lars James C. Blackmore of Caltech for NASA's Jet Propulsion Laboratory. For more information, contact [iaoffice@jpl.nasa.gov](mailto:iaoffice@jpl.nasa.gov). NPO-46962*

---

## Full Piezoelectric Multilayer-Stacked Hybrid Actuation/Transduction Systems

**Applications range from dynamic control and underwater detection to health monitoring and use in acoustic structures.**

*Langley Research Center, Hampton, Virginia*

The Stacked HYBATS (Hybrid Actuation/Transduction system) demonstrates significantly enhanced electromechanical performance by using the cooperative contributions of the electromechanical responses of multilayer, stacked negative strain components and positive strain components. Both experimental and theoretical studies indicate that, for Stacked HYBATS, the displacement is over three times that of a same-sized conventional flexensional actuator/transducer. The coupled resonance mode between positive strain and negative strain components of Stacked HY-

BATS is much stronger than the resonance of a single element actuation only when the effective lengths of the two kinds of elements match each other. Compared with the previously invented hybrid actuation system (HYBAS), the multilayer Stacked HYBATS can be designed to provide high mechanical load capability, low voltage driving, and a highly effective piezoelectric constant.

The negative strain component will contract, and the positive strain component will expand in the length directions when an electric field is applied on the device. The interaction between the two

elements makes an enhanced motion along the Z direction for Stacked-HYBATS. In order to dominate the dynamic length of Stacked-HYBATS by the negative strain component, the area of the cross-section for the negative strain component will be much larger than the total cross-section areas of the two positive strain components. The transverse strain is negative and longitudinal strain positive in inorganic materials, such as ceramics/single crystals. Different piezoelectric multilayer stack configurations can make a piezoelectric ceramic/single-crystal multilayer stack exhibit negative strain or

positive strain at a certain direction with-  
out increasing the applied voltage. The  
difference of this innovation from the  
HYBAS is that all the elements can be  
made from one-of-a-kind materials.

Stacked HYBATS can provide an ex-  
tremely effective piezoelectric constant  
at both resonance and off resonance fre-  
quencies. The effective piezoelectric

constant can be alternated by varying  
the size of each component, the degree  
of the pre-curvature of the positive strain  
components, the thickness of each layer  
in the multilayer stacks, and the piezo-  
electric constant of the material used.  
Because all of the elements are piezo-  
electric components, Stacked HYBATS  
can serve as projector and receiver for

underwater detection. The performance  
of this innovation can be enhanced by  
improving the piezoelectric properties.

*This work was done by Ji Su of Langley Re-  
search Center, Xiaoning Jiang of TSR Tech-  
nologies, and Tian-Bing Zu of the National  
Institute of Aerospace. Further information is  
contained in a TSP (see page 1). LAR-  
17671-1*

---

## Active Flow Effectors for Noise and Separation Control

**These variable effectors provide enhanced vehicle and aeroelastic control.**

*Langley Research Center, Hampton, Virginia*

New flow effector technology for separa-  
tion control and enhanced mixing is based  
upon shape memory alloy hybrid compos-  
ite (SMAHC) technology. The technology  
allows for variable shape control of aircraft  
structures through actively deformable sur-  
faces. The flow effectors are made by em-  
bedding shape memory alloy actuator ma-  
terial in a composite structure. When  
thermally actuated, the flow effector  
deflects into or out of the flow in a pre-  
scribed manner to enhance mixing or in-  
duce separation for a variety of applica-  
tions, including aeroacoustic noise  
reduction, drag reduction, and flight con-  
trol. The active flow effectors were devel-  
oped for noise reduction as an alternative  
to fixed-configuration effectors, such as

static chevrons, that cannot be optimized  
for airframe installation effects or variable  
operating conditions and cannot be re-  
tracted for off-design or fail-safe conditions.

Benefits include:

- Increased vehicle control, overall effi-  
ciency, and reduced noise throughout  
all flight regimes,
- Reduced flow noise,
- Reduced drag,
- Simplicity of design and fabrication,
- Simplicity of control through direct cur-  
rent stimulation, autonomous response  
to environmental heating, fast response,  
and a high degree of geometric stability.

The concept involves embedding pre-  
strained SMA actuators on one side of  
the chevron neutral axis in order to gen-

erate a thermal moment and deflect the  
structure out of plane when heated. The  
force developed in the host structure  
during deflection and the aerodynamic  
load is used for returning the structure  
to the retracted position. The chevron  
design is highly scalable and versatile,  
and easily affords active and/or auton-  
omous (environmental) control.

The technology offers wide-ranging  
market applications, including aero-  
space, automotive, and any application  
that requires flow separation or noise  
control.

*This work was done by Travis L. Turner of  
Langley Research Center. For further informa-  
tion, contact the Langley Innovative Partner-  
ships Office at (757) 864-8881. LAR-17332-1*

---

## Method and System for Temporal Filtering in Video Compression Systems

**This filtering improvement increases efficiency for visual signal components for low-power applications.**

*Stennis Space Center, Mississippi*

Three related innovations combine  
improved non-linear motion estima-  
tion, video coding, and video compres-  
sion. The first system comprises a  
method in which side information is  
generated using an adaptive, non-linear  
motion model. This method enables ex-  
trapolating and interpolating a visual  
signal, including determining the first  
motion vector between the first pixel  
position in a first image to a second  
pixel position in a second image; deter-  
mining a second motion vector between  
the second pixel position in the second  
image and a third pixel position in a  
third image; determining a third mo-

tion vector between the first pixel posi-  
tion in the first image and the second  
pixel position in the second image, the  
second pixel position in the second  
image, and the third pixel position in  
the third image using a non-linear  
model; and determining a position of  
the fourth pixel in a fourth image based  
upon the third motion vector.

For the video compression element,  
the video encoder has low computa-  
tional complexity and high compres-  
sion efficiency. The disclosed system  
comprises a video encoder and a de-  
coder. The encoder converts the source  
frame into a space-frequency represen-

tation, estimates the conditional statis-  
tics of at least one vector of space-fre-  
quency coefficients with similar fre-  
quencies, and is conditioned on  
previously encoded data. It estimates an  
encoding rate based on the conditional  
statistics and applies a Slepian-Wolf  
code with the computed encoding rate.  
The method for decoding includes gen-  
erating a side-information vector of fre-  
quency coefficients based on previously  
decoded source data and encoder statis-  
tics and previous reconstructions of  
the source frequency vector. It also per-  
forms Slepian-Wolf decoding of a  
source frequency vector based on the

generated side-information and the Slepian-Wolf code bits.

The video coding element includes receiving a first reference frame having a first pixel value at a first pixel position, a second reference frame having a second pixel value at a second pixel position, and a third reference frame having a third pixel value at a third pixel position. It determines a first motion vector between the first pixel position and the second pixel position, a second motion vector be-

tween the second pixel position and the third pixel position, and a fourth pixel value for a fourth frame based upon a linear or nonlinear combination of the first pixel value, the second pixel value, and the third pixel value. A stationary filtering process determines the estimated pixel values. The parameters of the filter may be predetermined constants.

*This work was done by Ligang Lu, Drake He, Ashish Jagmohan, and Vadim Sheinin of IBM for Stennis Space Center.*

*Inquiries concerning rights for the commercial use of this invention should be addressed to:*

*IBM*

*1101 Kitchawan Road*

*Yorktown Heights, NY 10598*

*Telephone No. (914) 945-3114*

*E-mail: lul@us.ibm.com*

*Refer to SSC-00291/309/310, volume and number of this NASA Tech Briefs issue, and the page number.*

---

## Apparatus for Measuring Total Emissivity of Small, Low-Emissivity Samples

*Goddard Space Flight Center, Greenbelt, Maryland*

An apparatus was developed for measuring total emissivity of small, lightweight, low-emissivity samples at low temperatures. The entire apparatus fits inside a small laboratory cryostat. Sample installation and removal are relatively quick, allowing for faster testing.

The small chamber surrounding the sample is lined with black-painted aluminum honeycomb, which simplifies data analysis. This results in the sample viewing a very high-emissivity surface on all sides, an effect which would normally require a much larger chamber volume. The sample and chamber temperatures are indi-

vidually controlled using off-the-shelf PID (proportional-integral-derivative) controllers, allowing flexibility in the test conditions. The chamber can be controlled at a higher temperature than the sample, allowing a direct absorptivity measurement.

The lightweight sample is suspended by its heater and thermometer leads from an isothermal bar external to the chamber. The wires run out of the chamber through small holes in its corners, and the wires do not contact the chamber itself. During a steady-state measurement, the thermometer and bar are individually controlled at the same temperature, so

there is zero heat flow through the wires. Thus, all of sample-temperature-control heater power is radiated to the chamber.

Double-aluminized Kapton (DAK) emissivity was studied down to 10 K, which was about 25 K colder than any previously reported measurements. This verified a minimum in the emissivity at about 35 K and a rise as the temperature dropped to lower values.

*This work was done by James Tuttle and Michael J. DiPirro of Goddard Space Flight Center. For further information, contact the Goddard Innovative Partnerships Office at (301) 286-5810. GSC-15697-1*

---

## Multiple-Zone Diffractive Optic Element for Laser Ranging Applications

**This technology can be used on unmanned aerial vehicles, or in collision-avoidance and robotic control applications in cars, trains, and ships.**

*Goddard Space Flight Center, Greenbelt, Maryland*

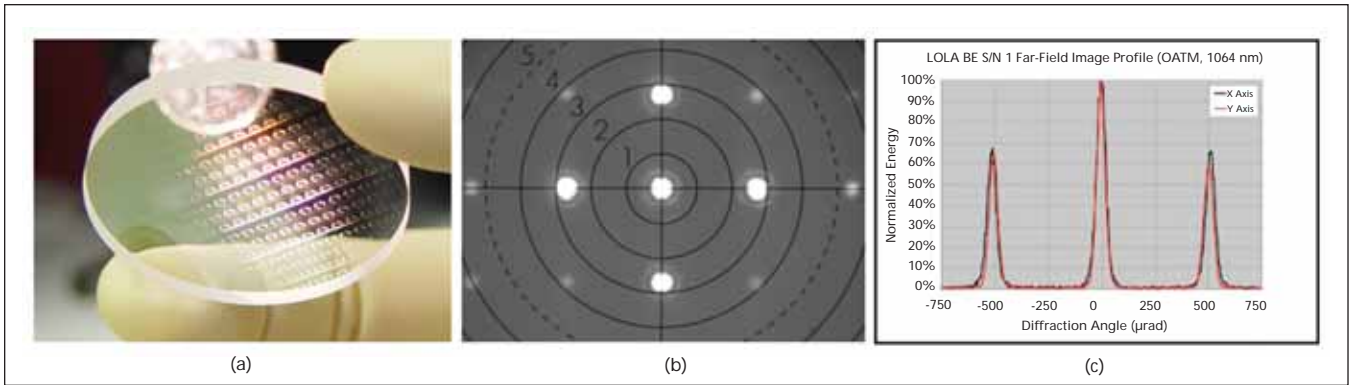
A diffractive optic element (DOE) can be used as a beam splitter to generate multiple laser beams from a single input laser beam. This technology has been recently used in LRO's Lunar Orbiter Laser Altimeter (LOLA) instrument to generate five laser beams that measure the lunar topography from a 50-km nominal mapping orbit (see figure). An extension of this approach is to use a multiple-zone DOE to allow a laser altimeter instrument to operate over a wider range of distances. In particular, a multiple-zone DOE could be used for applications that require both mapping and landing on a planetary body. In this

case, the laser altimeter operating range would need to extend from several hundred kilometers down to a few meters.

The innovator was recently involved in an investigation how to modify the LOLA instrument for the OSIRIS asteroid mapping and sample return mission. One approach is to replace the DOE in the LOLA laser beam expander assembly with a multiple-zone DOE that would allow for the simultaneous illumination of the asteroid with mapping and landing laser beams. The proposed OSIRIS multiple-zone DOE would generate the same LOLA five-beam output pattern for high-altitude topographic mapping, but

would simultaneously generate a wide divergence angle beam using a small portion of the total laser energy for the approach and landing portion of the mission. Only a few percent of the total laser energy is required for approach and landing operations as the return signal increases as the inverse square of the ranging height. A wide divergence beam could be implemented by making the center of the DOE a diffractive or refractive negative lens. The beam energy and beam divergence characteristics of a multiple-zone DOE could be easily tailored to meet the requirements of other missions that require laser ranging data.





LOLA DOE: (a) Picture, (b) Far-field image, and (c) Image normalized cross-section.

Current single-zone DOE lithographic manufacturing techniques could also be used to fabricate a multiple-zone DOE by masking the different DOE zones during the manufacturing process, and the same space-compatible DOE substrates (fused silica, sapphire) that are used on standard DOE's could be used for multiple-zone DOE's.

DOEs are an elegant and cost-effective optical design option for space-

based laser altimeters that require multiple output laser beams. The use of multiple-zone DOEs would allow for the design and optimization of a laser altimeter instrument required to operate over a large range of target distances, such as those designed to both map and land on a planetary body. In addition to space-based laser altimeters, this technology could find applications in military or commercial unmanned

aerial vehicles (UAVs) that fly at an altitude of several kilometers and need to land. It is also conceivable that variations of this approach could be used in land-based applications such as collision avoidance and robotic control of cars, trains, and ships.

*This work was done by Luis A. Ramos-Izquierdo of Goddard Space Flight Center. Further information is contained in a TSP (see page 1). GSC-15620-1*

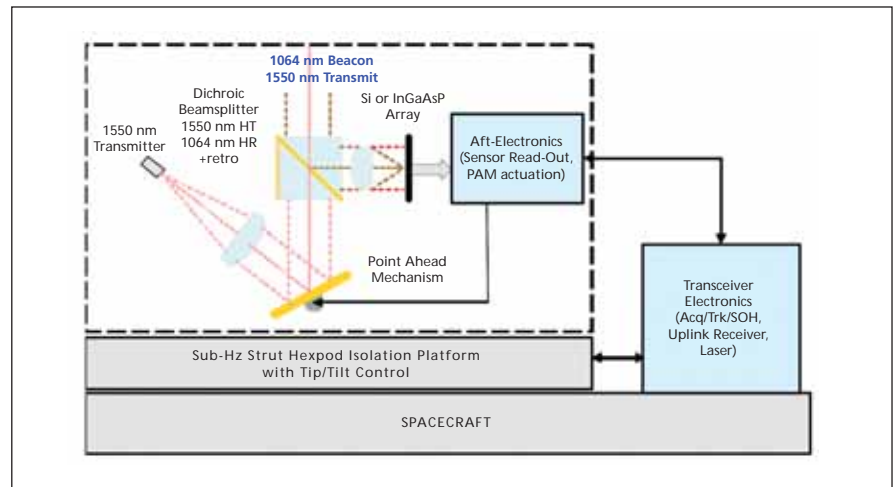
## Simplified Architecture for Precise Aiming of a Deep-Space Communication Laser Transceiver

**New optical transceiver is a combination of innovative technologies.**

*NASA's Jet Propulsion Laboratory, Pasadena, California*

The simplified architecture is a minimal system for a deep-space optical communications transceiver. For a deep-space optical communications link the simplest form of the transceiver requires (1) an efficient modulated optical source, (2) a point-ahead mechanism (PAM) to compensate for two-way light travel, (3) an aperture to reduce the divergence of the transmit laser communication signal and also to collect the uplink communication signal, and (4) a receive detector to sense the uplink communication signal. Additional components are introduced to mitigate for spacecraft microvibrations and to improve the pointing accuracy.

The Canonical Transceiver implements this simplified architecture (see figure). A single photon-counting "smart focal plane" sensor combines acquisition, tracking, and forward link data detection functionality. This improves optical efficiency by eliminating channel splits. A transmit laser blind sensor (e.g. silicon with 1,550-nm beam) provides transmit beam-pointing feedback via the



The Canonical Transceiver Architecture simplifies the design of the deep-space optical transceiver. Innovative technologies enabling its implementation include a single photon-counting detector array, two-photon absorption downlink tracking, a low-power point-ahead mechanism, and a sub-Hertz vibration isolation platform.

two-photon absorption (TPA) process. This vastly improves the transmit/receive isolation because only the focused transmit beam is detected. A piezoelectric tip-tilt actuator implements the required

point-ahead angle. This point-ahead mechanism has been demonstrated to have near zero quiescent power and is flight qualified. This architecture also uses an innovative 100-mHz resonant fre-

quency passive isolation platform to filter spacecraft vibrations with voice coil actuators for active tip-tilt correction below the resonant frequency.

The canonical deep-space optical communications transceiver makes synergistic use of innovative technologies to

reduce size, weight, power, and cost. This optical transceiver can be used to retire risks associated with deep-space optical communications on a planetary pathfinder mission and is complementary to ongoing lunar and access link developments.

*This work was done by Gerard G. Ortiz, William H. Farr, and Jeffrey R. Charles of Caltech for NASA's Jet Propulsion Laboratory. Further information is contained in a TSP (see page 1). NPO-46073*

## Two-Photon-Absorption Scheme for Optical Beam Tracking

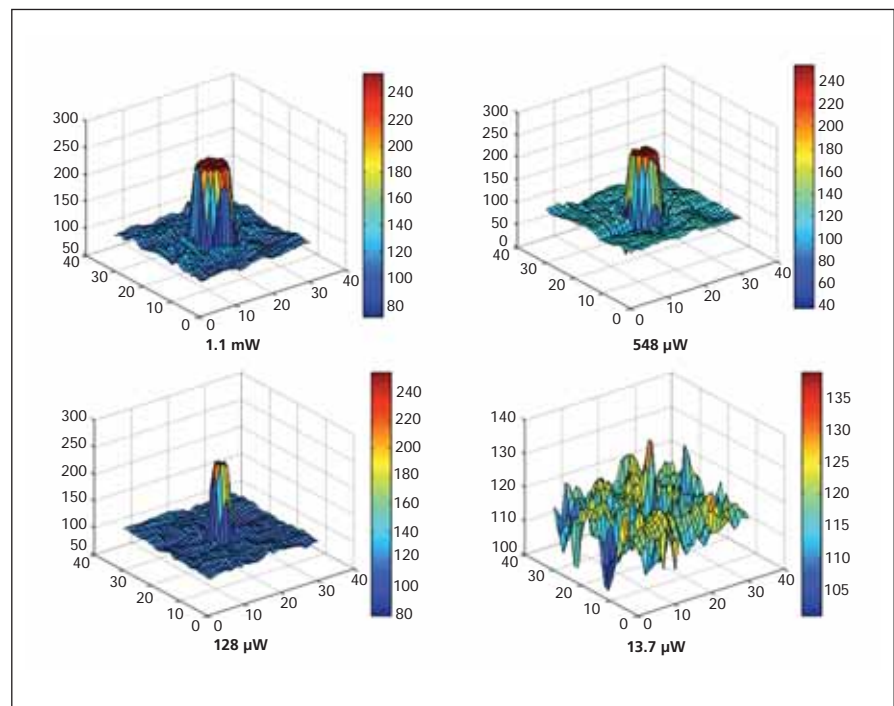
**This approach reduces cost for free-space optical communication receivers.**

*NASA's Jet Propulsion Laboratory, Pasadena, California*

A new optical beam tracking approach for free-space optical communication links using two-photon absorption (TPA) in a high-bandgap detector material was demonstrated. This tracking scheme is part of the canonical architecture described in the preceding article. TPA is used to track a long-wavelength transmit laser while direct absorption on the same sensor simultaneously tracks a shorter-wavelength beacon. The TPA responsivity was measured for silicon using a PIN photodiode at a laser beacon wavelength of 1,550 nm. As expected, the responsivity shows a linear dependence with incident power level. The responsivity slope is  $4.5 \times 10^{-7}$  A/W<sup>2</sup>. Also, optical beam spots from the 1,550-nm laser beacon were characterized on commercial charge-coupled device (CCD) and complementary metal-oxide semiconductor (CMOS) imagers with as little as 13.7  $\mu$ W of optical power (see figure). This new tracker technology offers an innovative solution to reduce system complexity, improve transmit/receive isolation, improve optical efficiency, improve signal-to-noise ratio (SNR), and reduce cost for free-space optical communications transceivers.

*This work was done by Gerardo G. Ortiz and William H. Farr of Caltech for NASA's Jet Propulsion Laboratory. Further informa-*

*tion is contained in a TSP (see page 1). NPO-46063*



**Two-Photon Absorption** generated signal levels caused by a 1,550 nm laser focused spot on a silicon CMOS focal plane array detector at various power levels. Note that the spot is distinguishable even with incident power levels in the 10's of microwatts.

## High-Sensitivity, Broad-Range Vacuum Gauge Using Nanotubes for Micromachined Cavities

*NASA's Jet Propulsion Laboratory, Pasadena, California*

A broad-range vacuum gauge has been created by suspending a single-walled carbon nanotube (SWNT) (metallic or semiconducting) in a Schottky diode format or in a bridge conductor format, between two electrically charged mesas. SWNTs are highly sensitive to molecular collisions because of

their extremely small diameters in the range of 1 to 3 nanometers. The measurement parameter will be the change in conductivity of SWNT due to decreasing rate of molecular collisions as the pressure inside a chamber decreases.

The rate of heat removal approaches a saturation limit as the mean free path

(m.f.p.) lengths of molecules increase due to decreasing pressure. Only those sensing elements that have a long relaxation time can produce a measurable response when m.f.p. of molecules increases (or time between two consecutive collisions increases). A suspended SWNT offers such a capability because

of its one-dimensional nature and ultra-small diameter. In the initial approach, similar architecture was used as that of a SWNT-Schottky diode that has been developed at JPL, and has its changing conductivity measured as the test chamber is pumped down from atmospheric pressure to high vacuum ( $10^{-7}$  Torr). Continuous response of decreasing conductivity has been measured as a function of decreasing pressure (SWNT is a

negative thermal coefficient material) from atmosphere to  $<10^{-6}$  Torr. A measurable current change in the hundreds of nA range has been recorded in the  $10^{-6}$  Torr regime.

*This work was done by Harish Manohara and Anupama B. Kaul of Caltech for NASA's Jet Propulsion Laboratory. For more information, contact iaoffice@jpl.nasa.gov.*

*In accordance with Public Law 96-517, the contractor has elected to retain title to this*

*invention. Inquiries concerning rights for its commercial use should be addressed to:*

*Innovative Technology Assets Management  
JPL*

*Mail Stop 202-233*

*4800 Oak Grove Drive*

*Pasadena, CA 91109-8099*

*E-mail: iaoffice@jpl.nasa.gov*

*Refer to NPO-45383, volume and number of this NASA Tech Briefs issue, and the page number.*

## Wide-Field Optic for Autonomous Acquisition of Laser Link

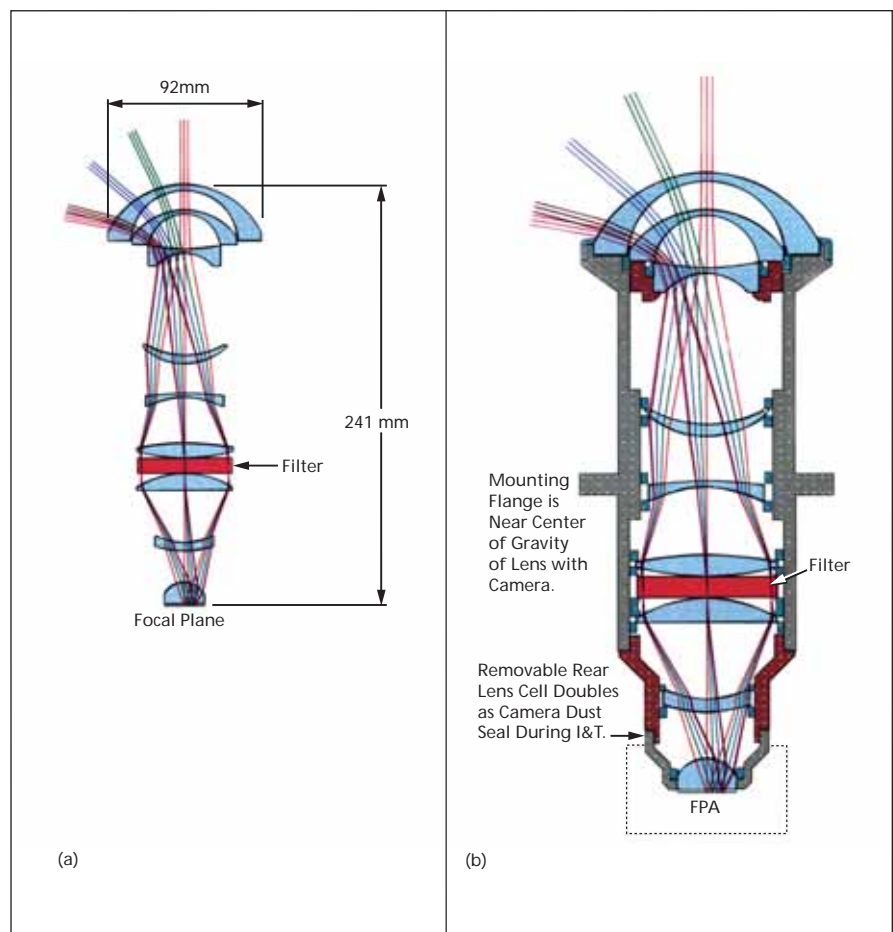
**This system has application in conventional wide-angle imaging such as low-light cockpit imaging, and in long-range motion detection.**

*NASA's Jet Propulsion Laboratory, Pasadena, California*

An innovation reported in "Two-Camera Acquisition and Tracking of a Flying Target," *NASA Tech Briefs*, Vol. 32, No. 8 (August 2008), p. 20, used a commercial fish-eye lens and an electronic imaging camera for initially locating objects with subsequent handover to an actuated narrow-field camera. But this operated against a dark-sky background. An improved solution involves an optical design based on custom optical components for the wide-field optical system that directly addresses the key limitations in acquiring a laser signal from a moving source such as an aircraft or a spacecraft.

The first challenge was to increase the light collection entrance aperture diameter, which was approximately 1 mm in the first prototype. The new design presented here increases this entrance aperture diameter to 4.2 mm, which is equivalent to a more than 16 times larger collection area. One of the trades made in realizing this improvement was to restrict the field-of-view to  $+80^\circ$  elevation and  $360^\circ$  azimuth. This trade stems from practical considerations where laser beam propagation over the excessively high air mass, which is in the line of sight (LOS) at low elevation angles, results in vulnerability to severe atmospheric turbulence and attenuation. An additional benefit of the new design is that the large entrance aperture is maintained even at large off-axis angles when the optic is pointed at zenith.

The second critical limitation for implementing spectral filtering in the design was tackled by collimating the light prior to focusing it onto the focal plane. This allows the placement of the narrow spectral filter in the collimated portion of the



(a) The custom optical design and ray-trace of the Wide-Field Optical Assembly; and (b) a Conceptual Optomechanical Design for holding the optical components and providing interface to the focal plane array (FPA). The collected light is substantially collimated prior to being passed through the spectral filter.

beam. For the narrow band spectral filter to function properly, it is necessary to adequately control the range of incident angles at which received light intercepts the filter. When this angle is restricted via collimation, narrower spectral filtering can

be implemented. The collimated beam (and the filter) must be relatively large to reduce the incident angle down to only a few degrees. In the presented embodiment, the filter diameter is more than ten times larger than the entrance aperture.

Specifically, the filter has a clear aperture of about 51 mm.

The optical design is refractive, and is comprised of nine custom refractive elements and an interference filter. The restricted maximum angle through the narrow-band filter ensures the efficient

use of a 2-nm noise equivalent bandwidth spectral width optical filter at low elevation angles (where the range is longest), at the expense of less efficiency for high elevations, which can be tolerated because the range at high elevation angles is shorter. The image circle is 12

mm in diameter, mapped to  $80 \times 360^\circ$  of sky, centered on the zenith.

*This work was done by Norman A. Page, Jeffrey R. Charles, and Abhijit Biswas of Caltech for NASA's Jet Propulsion Laboratory. Further information is contained in a TSP (see page 1). NPO-46945*

---

## Extracting Zero-Gravity Surface Figure of a Mirror

*NASA's Jet Propulsion Laboratory, Pasadena, California*

The technical innovation involves refinement of the classic optical technique of averaging surface measurements made in different orientations with respect to gravity, so the effects of gravity cancel in the averaged image. Particularly for large, thin mirrors subject to substantial deformation, the further requirement is that mount forces must also cancel when averaged over measurement orientations. The zero-gravity surface figure of a mirror in a hexapod mount is obtained by analyzing the summation of mount forces in

the frame of the optic as surface metrology is averaged over multiple clockings. This is illustrated with measurements taken from the Space Interferometry Mission (SIM) PT-M1 mirror for both twofold and threefold clocking. The positive results of these measurements and analyses indicate that, from this perspective, a lighter mirror could be used; that is, one might place less reliance on the damping effects of the elliptic partial differential equations that describe the propagation of forces through glass.

The advantage over prior art is relaxing the need for an otherwise substantial thickness of glass that might be needed to ensure accurate metrology in the absence of a detailed understanding and analysis of the mount forces. The general insights developed here are new, and provide the basic design principles on which mirror mount geometry may be chosen.

*This work was done by Eric E. Bloemhof, Jonathan C. Lam, V. Alfonso Fera, and Zensheu Chang of Caltech for NASA's Jet Propulsion Laboratory. For more information, contact [iaoffice@jpl.nasa.gov](mailto:iaoffice@jpl.nasa.gov). NPO-47259*



## Modeling Electromagnetic Scattering From Complex Inhomogeneous Objects

**Complex, inhomogeneous objects can be easily modeled using commercial CAD packages.**

*NASA Langley Research Center, Hampton, Virginia*

This software innovation is designed to develop a mathematical formulation to estimate the electromagnetic scattering characteristics of complex, inhomogeneous objects using the finite-element-method (FEM) and method-of-moments (MoM) concepts, as well as to develop a FORTRAN code called FEMOM3DS (Finite Element Method and Method of Moments for 3-Dimensional Scattering), which will implement the steps that are described in the mathematical formulation. Very complex objects can be easily modeled, and the operator of the code is not required to know the details of electromagnetic theory to study electromagnetic scattering.

Consider a complex inhomogeneous object geometry, the electromagnetic scattering characteristics of which are to be estimated when illuminated by a plane electromagnetic wave. To facilitate the mathematical formulation using the hybrid FEM/MoM, the object is assumed to be enclosed by a surface indicated as a fictitious outer boundary. Inside the boundary, the electromagnetic fields are obtained using the

FEM, whereas the electromagnetic fields outside the fictitious boundary are obtained using the assumed equivalent electric and magnetic currents flowing on the fictitious boundary. Continuity of the electromagnetic fields across the fictitious boundary results in partly sparse/dense matrix that is solved for the unknown fields inside the fictitious boundary including the boundary surface.

The steps laid out in the mathematical formulation are carried out in FEMOM3DS. Along with the main FEMOM3DS, the innovation uses a commercial computer-aided-design (CAD) package for geometrical modeling, and a post-processing package such as Techplot for displaying graphically the results obtained using FEMOM3DS. In the present FEMOM3DS code the COSMOS/M commercial software is used as a CAD tool to model the geometry of a given problem. The COSMOS/M is also used to discretize the FEM region using the tetrahedral elements. Various inhomogeneous regions are taken care of by having many parts in the FEM region. Using the COS-

MOS/M, common boundaries where boundary conditions are to be implemented are also identified. The data file created by the COSMOS/M for node and element information is then generated and processed through the preprocessor part of FEMOM3DS code to create edge information and node information. The preprocessed data are then run through the main part of FEMOM3DS to obtain electromagnetic scattering. The output files from the FEMOM3DS can be used for displaying the results in a graphical format.

The FEMOM3DS is written in FORTRAN 77. The code was successfully compiled on a CONVEX machine. However, the code can be compiled on any 32-bit machine like PCs or SUN, SGI UNIX Station. To get correct results, dimensions must be given in centimeters, frequency of operation must be given in GHz and incident and observation angles must be specified in degrees.

*This work was done by Manohar Deshpande and C. J. Reddy of Langley Research Center. Further information is contained in a TSP (see page 1). LAR-17090-1*

## Visual Object Recognition and Tracking of Tools

**This method can be used to track tools held and used by humans, such as surgical tools.**

*Lyndon B. Johnson Space Center, Houston, Texas*

A method has been created to automatically build an algorithm off-line, using computer-aided design (CAD) models, and to apply this at runtime. The object type is discriminated, and the position and orientation are identified. This system can work with a single image and can provide improved performance using multiple images provided from videos.

The spatial processing unit uses three stages: (1) segmentation; (2) initial type, pose, and geometry (ITPG) estimation;

and (3) refined type, pose, and geometry (RTPG) calculation. The image segmentation module files all the tools in an image and isolates them from the background. For this, the system uses edge-detection and thresholding to find the pixels that are part of a tool. After the pixels are identified, nearby pixels are grouped into blobs. These blobs represent the potential tools in the image and are the product of the segmentation algorithm.

The second module uses matched filtering (or template matching). This ap-

proach is used for condensing synthetic images using an image subspace that captures key information. Three degrees of orientation, three degrees of position, and any number of degrees of freedom in geometry change are included. To do this, a template-matching framework is applied. This framework uses an off-line system for calculating template images, measurement images, and the measurements of the template images. These results are used online to match segmented tools against the templates.

The final module is the RTPG processor. Its role is to find the exact states of the tools given initial conditions provided by the ITPG module. The requirement that the initial conditions exist allows this module to make use of a local search (whereas the ITPG module had global scope). To perform the local search, 3D model matching is used, where a synthetic image of the object is created and compared to the sensed data. The availability of low-cost PC graphics hardware allows rapid creation of synthetic images. In this approach, a function of orientation, distance, and articulation is defined

as a metric on the difference between the captured image and a synthetic image with an object in the given orientation, distance, and articulation. The synthetic image is created using a model that is looked up in an object-model database.

A composable software architecture is used for implementation. Video is first preprocessed to remove sensor anomalies (like dead pixels), and then is processed sequentially by a prioritized list of tracker-identifiers.

*This work was done by James English, Chu-Yin Chang, and Neil Tardella of Energid Technologies for Johnson Space Center.*

*Further information is contained in a TSP (see page 1).*

*In accordance with Public Law 96-517, the contractor has elected to retain title to this invention. Inquiries concerning rights for its commercial use should be addressed to:*

*Energid Technologies  
124 Mount Auburn Street  
Suite 200 North  
Cambridge, MA 02138  
Phone No.: (617) 401-7090  
Toll Free No.: (888) 547-4100*

*Refer to MSC-23947-1, volume and number of this NASA Tech Briefs issue, and the page number.*

---

## Method for Implementing Optical Phase Adjustment

*Goddard Space Flight Center, Greenbelt, Maryland*

A method has been developed to mechanically implement the optical phase shift by adjusting the polarization of the pump and probe beams in an NMOR (nonlinear magneto-optical rotation) magnetometer as the proper phase shift is necessary to induce self-oscillation. This innovation consists of mounting the pump beam on a ring that surrounds the atomic vapor sample. The propagation of the probe beam is per-

pendicular to that of the pump beam. The probe beam can be considered as defining the axis of a cylinder, while the pump beam is directed radially. The magnetic field to be measured defines a third vector, but it is also taken to lie along the cylinder axis. Both the pump and probe beams are polarized such that their electric field vectors are substantially perpendicular to the magnet field. By rotation of the ring supporting

the pump beam, its direction can be varied relative to the plane defined by the probe electric field and the magnetic field to be measured.

*This work was done by David C. Hovde of Southwest Sciences and Eric Corsini of the University of California, Berkeley, for Goddard Space Flight Center. For further information, contact the Goddard Innovative Partnerships Office at (301) 286-5810. GSC-15608-1*

---

## Visual SLAM Using Variance Grid Maps

**This algorithm is suitable for real-time navigation on irregular terrain.**

*NASA's Jet Propulsion Laboratory, Pasadena, California*

An algorithm denoted "Gamma-SLAM" performs further processing, in real time, of preprocessed digitized images acquired by a stereoscopic pair of electronic cameras aboard an off-road robotic ground vehicle to build accurate maps of the terrain and determine the location of the vehicle with respect to the maps. Part of the name of the algorithm reflects the fact that the process of building the maps and determining the location with respect to them is denoted "simultaneous localization and mapping" (SLAM). Most prior real-time SLAM algorithms have been limited in applicability to (1) systems equipped with scanning laser range finders as the primary sensors in (2) indoor environments (or relatively simply structured outdoor environments). The few prior vision-based

SLAM algorithms have been feature-based and not suitable for real-time applications and, hence, not suitable for autonomous navigation on irregularly structured terrain.

The Gamma-SLAM algorithm incorporates two key innovations:

- Visual odometry (in contradistinction to wheel odometry) is used to estimate the motion of the vehicle.
- An elevation variance map (in contradistinction to an occupancy or an elevation map) is used to represent the terrain.

The Gamma-SLAM algorithm makes use of a Rao-Blackwellized particle filter (RBPF) from Bayesian estimation theory for maintaining a distribution over poses and maps. The core idea of the RBPF approach is that the SLAM problem can be factored into two parts: (1) finding the distribution over robot tra-

jectories, and (2) finding the map conditioned on any given trajectory. The factorization involves the use of a particle filter in which each particle encodes both a possible trajectory and a map conditioned on that trajectory. The base estimate of the trajectory is derived from visual odometry, and the map conditioned on that trajectory is a Cartesian grid of elevation variances. In comparison with traditional occupancy or elevation grid maps, the grid elevation variance maps are much better for representing the structure of vegetated or rocky terrain.

*This work was done by Andrew B. Howard of Caltech and Tim K. Marks of the University of California San Diego for NASA's Jet Propulsion Laboratory. For more information, contact [iaoffice@jpl.nasa.gov](mailto:iaoffice@jpl.nasa.gov). NPO-46114*

---

## ➤ Rapid Calculation of Spacecraft Trajectories Using Efficient Taylor Series Integration

Software greatly accelerates the calculation of spacecraft trajectories.

*John H. Glenn Research Center, Cleveland, Ohio*

A variable-order, variable-step Taylor series integration algorithm was implemented in NASA Glenn's SNAP (Spacecraft N-body Analysis Program) code. SNAP is a high-fidelity trajectory propagation program that can propagate the trajectory of a spacecraft about virtually any body in the solar system. The Taylor series algorithm's very high order accuracy and excellent stability properties lead to large reductions in computer time relative to the code's existing 8th order Runge-Kutta scheme. Head-to-head comparison on near-Earth, lunar, Mars, and Europa missions showed that Taylor series integration is 15.8 times faster than Runge-Kutta on average, and is more accurate. These speedups were obtained for calculations involving central body, other body, thrust, and drag forces. Similar speedups have been obtained for calculations that include J2 spherical harmonic for central body gravitation. The algorithm includes a step size selection method that directly calculates

the step size and never requires a repeat step.

High-order Taylor series integration algorithms have been shown to provide major reductions in computer time over conventional integration methods in numerous scientific applications. The objective here was to directly implement Taylor series integration in an existing trajectory analysis code and demonstrate that large reductions in computer time (order of magnitude) could be achieved while simultaneously maintaining high accuracy.

This software greatly accelerates the calculation of spacecraft trajectories. At each time level, the spacecraft position, velocity, and mass are expanded in a high-order Taylor series whose coefficients are obtained through efficient differentiation arithmetic. This makes it possible to take very large time steps at minimal cost, resulting in large savings in computer time. The Taylor series algorithm is implemented primarily through three subroutines: (1) a driver routine that automatically intro-

duces auxiliary variables and sets up initial conditions and integrates; (2) a routine that calculates system reduced derivatives using recurrence relations for quotients and products; and (3) a routine that determines the step size and sums the series. The order of accuracy used in a trajectory calculation is arbitrary and can be set by the user. The algorithm directly calculates the motion of other planetary bodies and does not require ephemeris files (except to start the calculation). The code also runs with Taylor series and Runge-Kutta used interchangeably for different phases of a mission.

*This work was done by James R. Scott and Michael C. Martini of Glenn Research Center. Further information is contained in a TSP (see page 1).*

*Inquiries concerning rights for the commercial use of this invention should be addressed to NASA Glenn Research Center, Innovative Partnerships Office, Attn: Steve Fedor, Mail Stop 4-8, 21000 Brookpark Road, Cleveland, Ohio 44135. Refer to LEW-18445-1.*

---

## ➤ Efficient Kriging Algorithms

*Goddard Space Flight Center, Greenbelt, Maryland*

More efficient versions of an interpolation method, called kriging, have been introduced in order to reduce its traditionally high computational cost. Written in C++, these approaches were tested on both synthetic and real data.

Kriging is a best unbiased linear estimator and suitable for interpolation of scattered data points. Kriging has long been used in the geostatistic and mining

communities, but is now being researched for use in the image fusion of remotely sensed data. This allows a combination of data from various locations to be used to fill in any missing data from any single location.

To arrive at the faster algorithms, sparse SYMMLQ iterative solver, covariance tapering, Fast Multipole Methods (FMM), and nearest neigh-

bor searching techniques were used. These implementations were used when the coefficient matrix in the linear system is symmetric, but not necessarily positive-definite.

*This work was done by Nargess Memarsadeghi of Goddard Space Flight Center. For further information, contact the Goddard Innovative Partnerships Office at (301) 286-5810. GSC-15555-1*

---

## ➤ Predicting Spacecraft Trajectories by the WeavEncke Method

*Lyndon B. Johnson Space Center, Houston, Texas*

A combination of methods is proposed of predicting spacecraft trajectories that possibly include multiple maneuvers and/or perturbing accelerations, with greater speed, accuracy, and repeatability than were heretofore achievable. The

combination is denoted the WeavEncke method because it is based on unpublished studies by Jonathan Weaver of the orbit-prediction formulation of the noted astronomer Johann Franz Encke. Weaver evaluated a number of alternatives that

arise within that formulation, arriving at an orbit-predicting algorithm optimized for complex trajectory operations.

In the WeavEncke method, Encke's method of prediction of perturbed orbits is enhanced by application of mod-

ern numerical methods. Among these methods are efficient Kepler's-equation time-of-flight solutions and self-starting numerical integration with time as the independent variable. Self-starting numerical integration satisfies the require-

ments for accuracy, reproducibility, and efficiency (and, hence, speed). Self-starting numerical integration also supports fully analytic regulation of integration step sizes, thereby further increasing speed while maintaining accuracy.

*This work was done by Jonathan K. Weaver of Johnson Space Center and Daniel R. Adamo of United Space Alliance. For further information, contact the JSC Innovation Partnerships Office at (281) 483-3809. MSC-23802-1*

---

## ➤ An Augmentation of G-Guidance Algorithms

**This augmented algorithm can be used in small-body proximity operations utilizing model predictive control with a need for safety from surface-constraint uncertainty.**

*NASA's Jet Propulsion Laboratory, Pasadena, California*

The original G-Guidance algorithm provided an autonomous guidance and control policy for small-body proximity operations that took into account uncertainty and dynamics disturbances. However, there was a lack of robustness in regards to object proximity while in autonomous mode. The modified G-Guidance algorithm was augmented with a second operational mode that allows switching into a safety hover mode. This will cause a spacecraft to hover in place until a mission-planning algorithm can compute a safe new trajectory. No state or control constraints are violated. When a new, feasible state trajectory is calculated, the spacecraft will return to standard mode and maneuver toward the target. The main goal of this augmentation is to protect the spacecraft in the event that a landing surface or obstacle is closer or further than anticipated. The algorithm can be used for the miti-

gation of any unexpected trajectory or state changes that occur during standard mode operations.

In order to have the G-Guidance algorithm detect an unsafe condition, it required some modification. This modification provides a policy to safely maneuver the spacecraft between its current state and a desired target state while ensuring satisfaction of thruster and trajectory constraints, along with safety constraints. In standard mode, this modification brings the spacecraft from its current position closer to its target state. In safety mode, the algorithm maintains the spacecraft's current state at zero velocity. Since the safety mode is designed to be temporary, the destination location in this mode is also temporary, and once a new destination location is provided, the spacecraft returns to standard mode.

The G-Guidance algorithm uses both a planned trajectory (feedforward) and

a control policy (feedback), along with sensors to monitor actual spacecraft state. The feedback is designed to ensure that the spacecraft stays within a specified proximity to the feedforward. The feedforward is designed to achieve the goals of each mode: hover for safety mode and maneuver toward target for standard mode. By giving the spacecraft the ability to re-compute its trajectory on-the-fly in response to local conditions, minimization of fuel usage is provided. The original G-Guidance algorithm provides robustness to uncertainty affecting the dynamics. The safety augmentation provides a form of state-constraint robustness, which further mitigates risk.

*This work was done by John M. Carson III and Behcet Acikmese of Caltech for NASA's Jet Propulsion Laboratory. For more information, contact [iaoffice@jpl.nasa.gov](mailto:iaoffice@jpl.nasa.gov). NPO-46452*

---

## ➤ Comparison of Aircraft Icing Growth Assessment Software

**The goal is to provide software that can predict ice growth under any condition for any aircraft surface.**

*John H. Glenn Research Center, Cleveland, Ohio*

A research project is underway to produce computer software that can accurately predict ice growth under any meteorological conditions for any aircraft surface. An extensive comparison of the results in a quantifiable manner against the database of ice shapes that have been generated in the NASA Glenn Icing Research Tunnel (IRT) has been performed, including additional data taken to extend the database in the Super-cooled Large Drop (SLD) regime. The project shows the differences in ice shape between LEWICE 3.2.2, GlenNICE, and experimental data.

The Icing Branch at NASA Glenn has produced several computer codes over the last 20 years for performing icing simulation. While some of these tools have been collaborative projects, most have been developed primarily by one person, with some assistance by others. The state of computing has also changed dramatically in that time period. As these codes have grown in complexity and have been accepted by users as production icing tools, there has arisen a need for the developers to adhere to standard software practices used to develop commercial software.

The project addresses the validation of the software against a recent set of ice-shape data in the SLD regime. This validation effort mirrors a similar effort undertaken for previous validations of LEWICE. Those reports quantified the ice accretion prediction capabilities of the LEWICE software. Several ice geometry features were proposed for comparing ice shapes in a quantitative manner. The resulting analysis showed that LEWICE compared well to the available experimental data.

The effects of super-cooled large droplets in icing have been researched



extensively since 1994. Since then, several experimental efforts have been made to document SLD ice shapes and to investigate the underlying physics. While this project provides comparisons to standard icing conditions, the empha-

sis was placed on the newer data, which is predominately SLD.

*This work was done by William Wright, Mark G. Potapczuk, and Laurie H. Levinson of Glenn Research Center. Further information is contained in a TSP (see page 1).*

*Inquiries concerning rights for the commercial use of this invention should be addressed to NASA Glenn Research Center, Innovative Partnerships Office, Attn: Steve Fedor, Mail Stop 4-8, 21000 Brookpark Road, Cleveland, Ohio 44135. Refer to LEW-18451-1.*





### **Silicon-Germanium Voltage-Controlled Oscillator at 105 GHz**

A group at UCLA, in collaboration with the Jet Propulsion Laboratory, has designed a voltage-controlled oscillator (VCO) created specifically for a compact, integrated, electronically tunable frequency generator useable for submillimeter-wave science instruments operating in extreme cold environments. The VCO makes use of SiGe heterojunction bipolar transistors (HBTs). The SiGe HBTs have a 0.13-micrometer emitter width. A differential design was used with two VCOs connected to form a quadrature signal. A 2.5-V supply is required to power the circuit. A cross-coupled CMOS pair is used for emitter-degeneration of the SiGe HBTs, and the design uses coupled load and base inductors. The circuit oscillates at 105 GHz. A linear superposition of VCOs has been designed to achieve four times the oscillation frequency of the fundamental oscillator.

*This work was done by Alden Wong, Tim Larocca, and M. Frank Chang of UCLA, and Lorene A. Samoska of Caltech for NASA's Jet Propulsion Laboratory. Further information is contained in a TSP (see page 1). NPO-47116*

### **Estimation of Coriolis Force and Torque Acting on Ares-1**

A document describes work on the origin of Coriolis force and estimating Coriolis force and torque applied to the Ares-1 vehicle during its ascent, based on an internal ballistics model for a multi-segmented solid rocket booster (SRB).

The work estimates Coriolis force and torque applied to the vehicle during its ascent. Maveric flight simulation software was used to produce the required angular velocity data for the Coriolis force and torque computations. For the simulation of gas movement in SRB, software was developed using a dynamical model of internal ballistics of the five-segmented SRB. Also included in the work are a study and estimate of Coriolis force and

torque applied to the rocket due to SRB nozzle movement. For calculation of internal ballistics, Coriolis force, and torque computations, MATLAB software was used.

Coriolis force and torque were calculated and applied to Ares-1 during its ascent. Two cases were considered: Coriolis force and torque applied to the rocket originating from gas movement in SRB, and Coriolis force and torque originating from exhaust gas movement in SRB nozzle. Coriolis force and torque are the largest during the first 20 seconds after the launch when rocket angular velocity is large. SRB Coriolis force is about 5.4 times larger than nozzle Coriolis force, and SRB Coriolis torque is about 2.8 times larger than the nozzle Coriolis torque at the time  $t=10$  seconds. The inclusion of flexible rocket model does not provide a significant change to the results of Coriolis force and torque computations in comparison with a rigid rocket model.

*This work was done by Ryan M. Mackey and Igor K. Kulikov of Caltech; Vadim Smelyanskiy and Dmitry Luchinsky of Ames Research Center; and Jeb Orr of BD Systems Inc. for NASA's Jet Propulsion Laboratory. Further information is contained in a TSP (see page 1).*

*The software used in this innovation is available for commercial licensing. Please contact Daniel Broderick of the California Institute of Technology at [danielb@caltech.edu](mailto:danielb@caltech.edu). Refer to NPO-47326.*

### **Null Lens Assembly for X-Ray Mirror Segments**

A document discusses a null lens assembly that allows laser interferometry of 60° slumped glass mirror segments used in x-ray mirrors. The assembly consists of four lenses in precise alignment to each other, with incorporated piezoelectric nanometer stepping actuators to position the lenses in six degrees of freedom for positioning relative to each other.

Each lens is first installed and epoxied into a 410 stainless steel "cell." The outer housing is designed to allow five degrees

of freedom of the lens. The cell is placed onto a 3/8-in. ( $\approx 9$ -mm) ball bearing in the base of the housing, which provides a pivot point for the rotations, and allows slight  $x$  and  $y$  translations (microns) by allowing the cell to slide against it. Rotations are accomplished by 5 commercial picomotors that push on the cell in 30-nanometer increments. Spring plungers on the opposite side of the cell from the picomotors secure the cell in the housing.

The 410 stainless steel is used for the cell, baseplate, and rails because it has a low CTE (coefficient of thermal expansion) relative to most other metals. It is used exclusively in the "growth path" of the optical assembly so that when bulk temperature changes occur in the lab, the lenses will move a consistent amount apart from each other (which is a less sensitive factor in alignment), but will not tilt or rotate (alignment is very sensitive to rotations).

*This work was done by David W. Robinson of Goddard Space Flight Center. Further information is contained in a TSP (see page 1). GSC 15790-1*

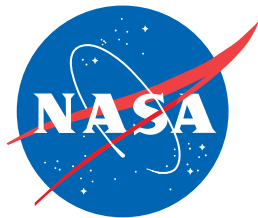
### **High-Precision Pulse Generator**

A document discusses a pulse generator with subnanosecond resolution implemented with a low-cost field-programmable gate array (FPGA) at low power levels. The method used exploits the fast carry chains of certain FPGAs. Prototypes have been built and tested in both Actel AX and Xilinx Virtex 4 technologies. In-flight calibration or control can be performed by using a similar and related technique as a time interval measurement circuit by measuring a period of the stable oscillator, as the delays through the fast carry chains will vary as a result of manufacturing variances as well as the result of environmental conditions (voltage, aging, temperature, and radiation).

*This work was done by Richard Katz and Igor Kleyner of Goddard Space Flight Center. Further information is contained in a TSP (see page 1). GSC- 15831-1*







National Aeronautics and  
Space Administration